Strong final state interactions seen by femtoscopy

Hanna Paulina Zbroszczyk

Warsaw University of Technology; Faculty of Physics

e-mail: *hanna.zbroszczyk@pw.edu.pl*

Faculty of Physics, University of Warsaw, 1 June 2023

Outline

Introduction

- QCD phase diagram
- HIC and femtoscopy method

Results

1. Interactions

a) Strong **interactions** between (anti)baryons

b) Motivation to Y-N and Y-Y **correlations**

c) Femtoscopy of **strange baryons** and their interactions

d) Possible **bound states**

e) **Coalescence** production of deuterons

f) **Nonidentical** particle correlation

2. QCD Phase diagram scan

Summary and conclusions

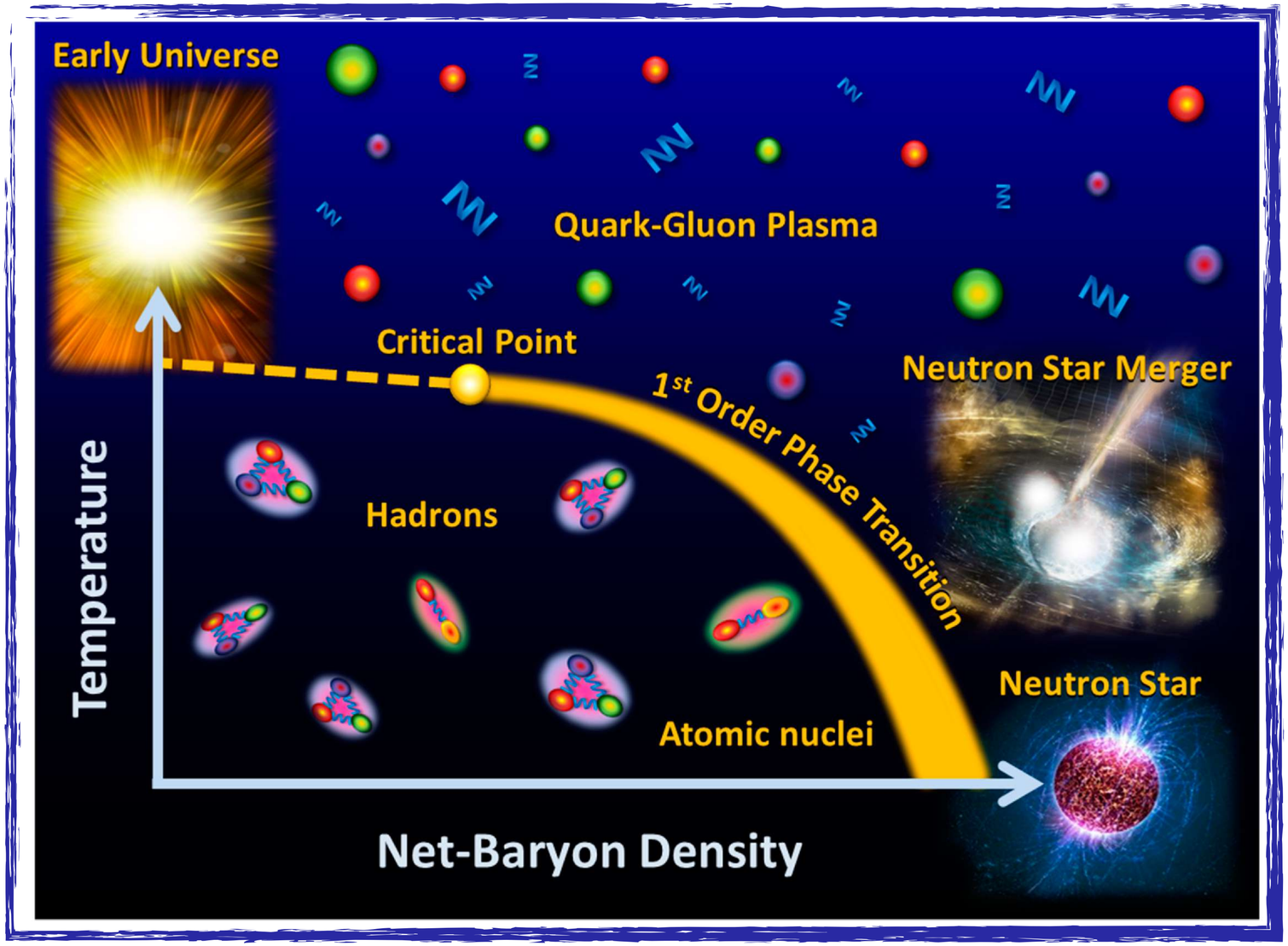

https://www.researchgate.net/figure/Color-Online-A-schematic-of-QCD-phase-diagram_fig2_357552969

Introduction

QCD Phase diagram of strongly interacting matter

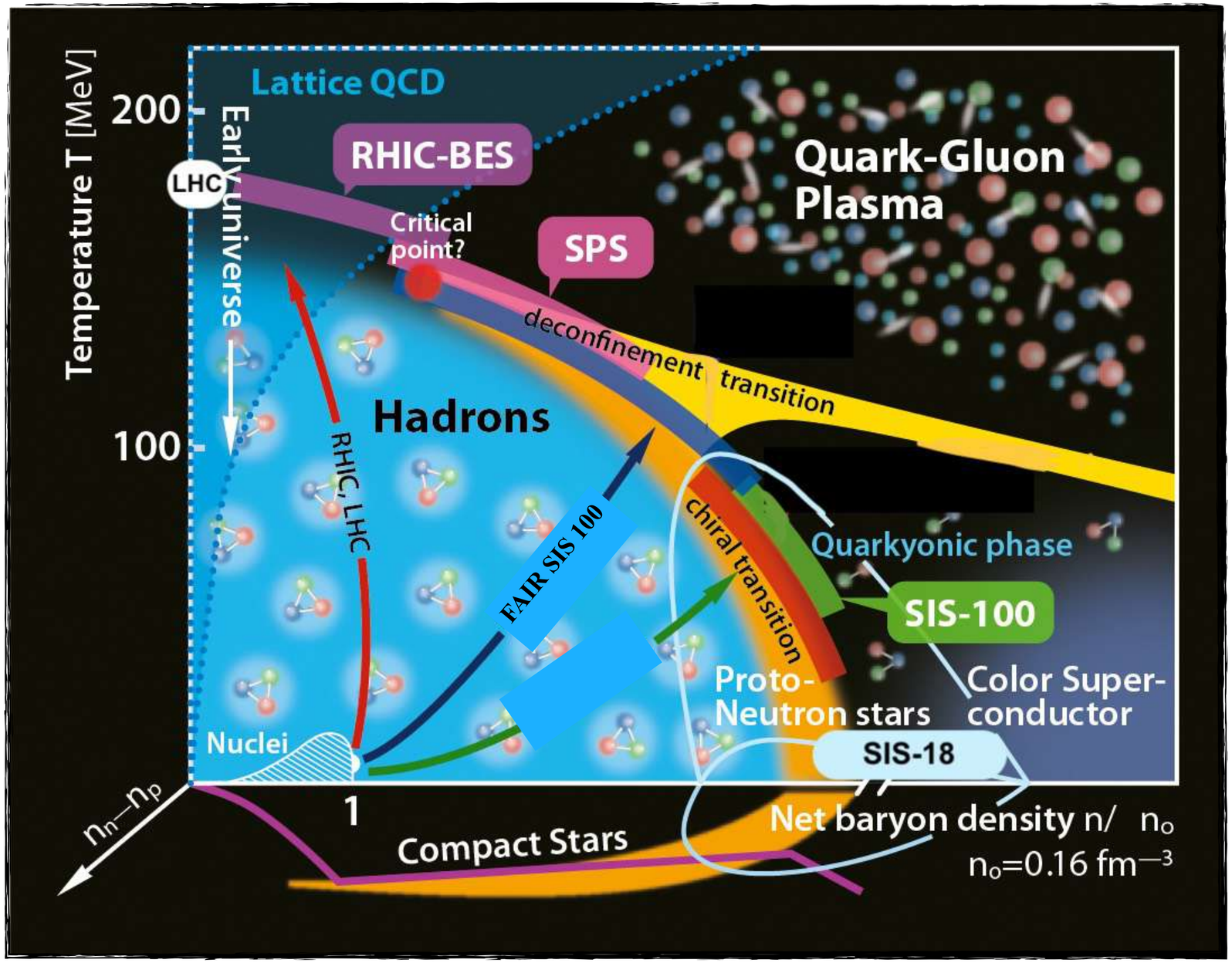

Heavy-Ion collision and the HBT method

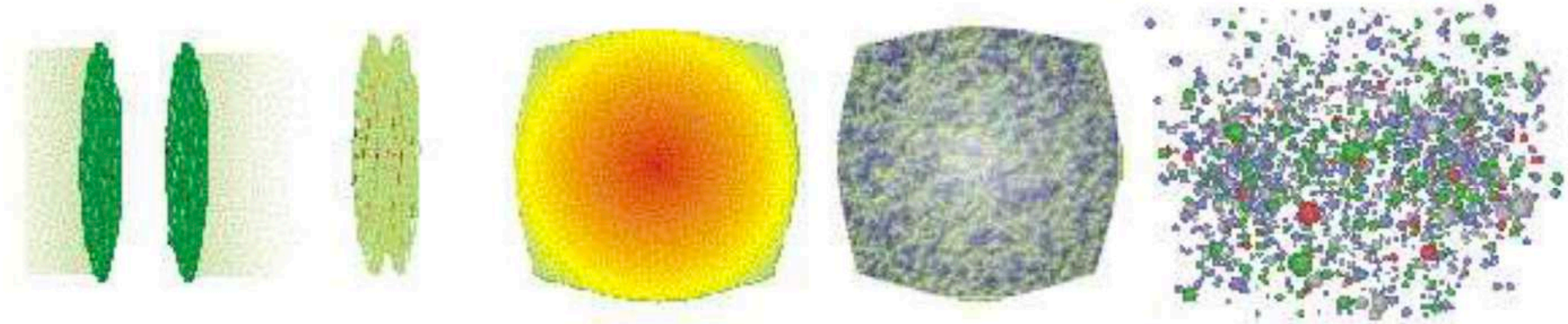

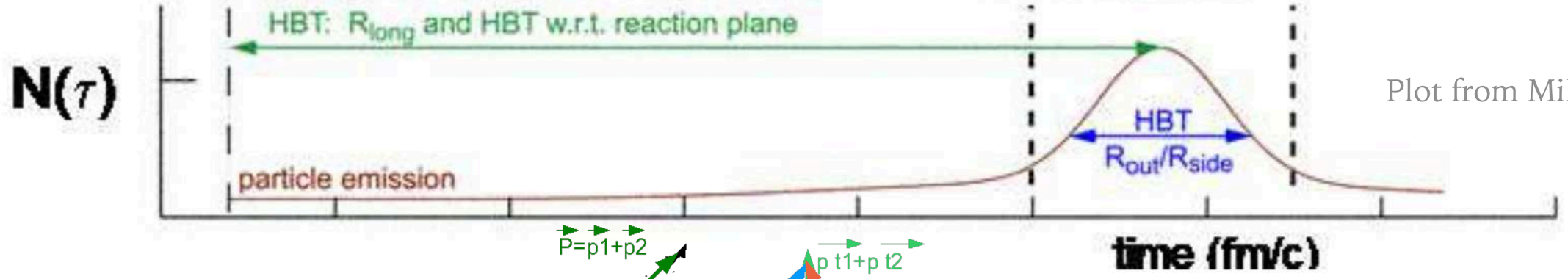

Plot from Mike Lisa

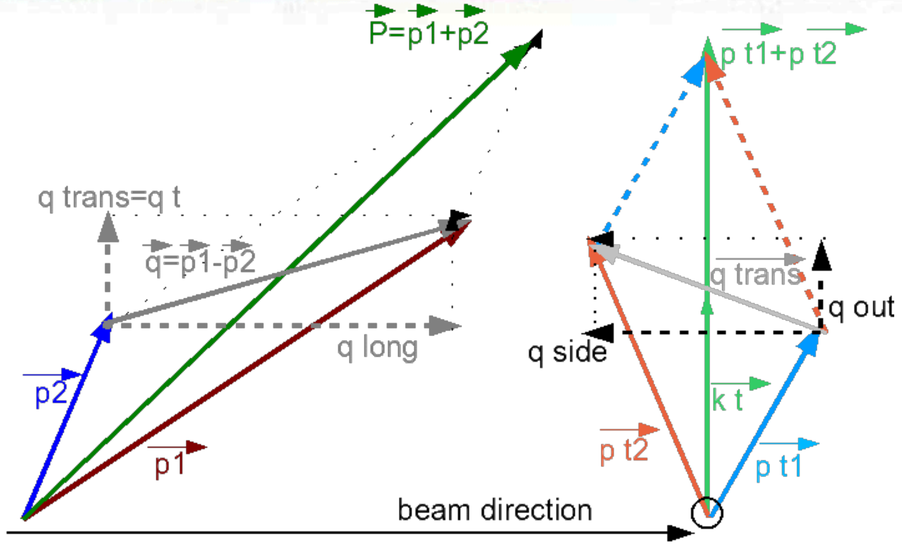

long - beam axis
out - pair transverse **p**
side - perpendicular to out and long

Correlation femtoscopy

Size: ~10^{-15} m (fm)
Time: ~10^{-23} s

Impossible
to measure directly!

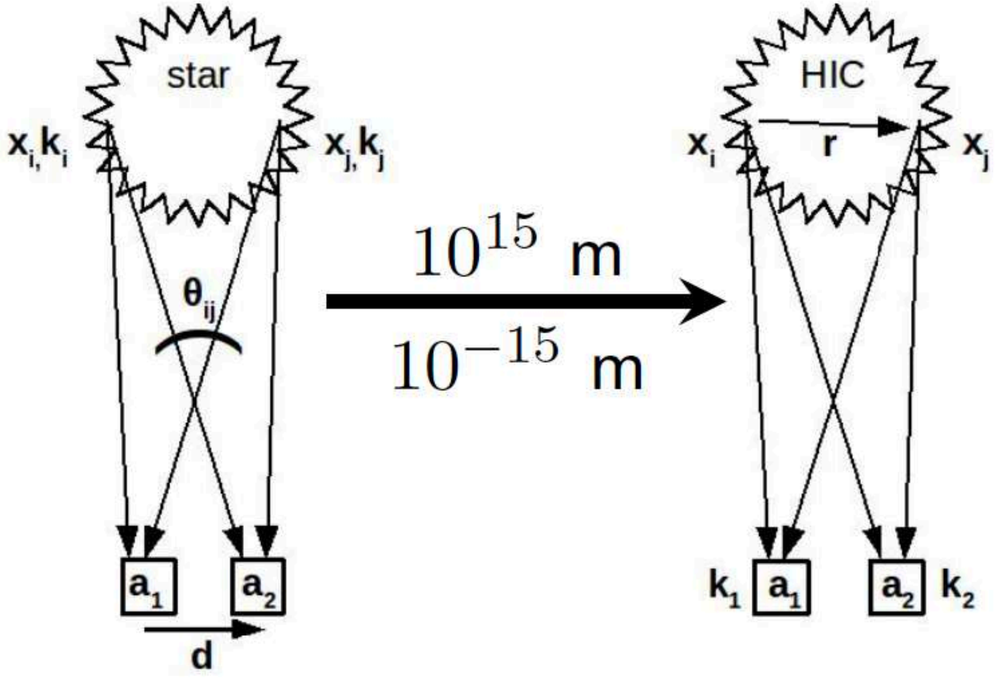

Femtoscopy (HIC) inspired by Hanbury Brown and Twiss interferometry method (Astronomy)

but!

- different scales,
- different measured quantities
- different determined quantities

Traditional and non-traditional femtoscopy

Femtoscopy (originating from HBT):
the method to probe **geometric** and **dynamic** properties of the source

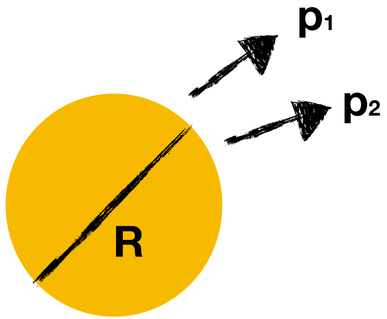

Space-time properties ($10^{-15}m$, $10^{-23}s$) can be determined due to two-particle correlations that arise due to:

Quantum Statistics (Fermi-Dirac, Bose-Einstein);

Final State Interactions (Coulomb, strong)

$$C(k^*, r^*) = \int S(r^*) \, |\Psi(k^*, r^*)|^2 \, d^3r^* = \frac{Sgnl(k^*)}{Bckg(k^*)}$$

(determined: $S(r^*)$; assumed: $\Psi(k^*, r^*)$; measured: $\frac{Sgnl(k^*)}{Bckg(k^*)}$)

$S(r^*)$ – emission function

$\Psi(k^*, r^*)$ – two-particle wave function (includes e.g. FSI interactions)

$\frac{Sgnl(k^*)}{Bckg(k^*)}$ – correlation function

Traditional and non-traditional femtoscopy

If we assume we know the **emission function**, measured **correlation function** can be used to determine **parameters** of **Final State Interactions**

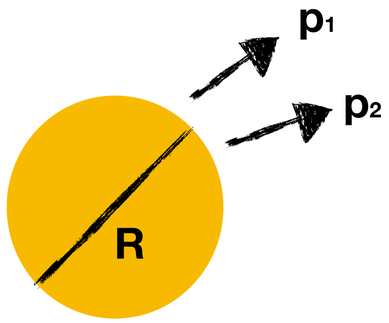

Space-time properties ($10^{-15}m$, $10^{-23}s$) can be determined due to two-particle correlations that arise due to:

Quantum Statistics (Fermi-Dirac, Bose-Einstein);

Final State Interactions (Coulomb, strong)

$$C(k^*, r^*) = \int S(r^*) \, |\Psi(k^*, r^*)|^2 \, d^3r^* = \frac{Sgnl(k^*)}{Bckg(k^*)}$$

assumed: $S(r^*)$ — determined: $\Psi(k^*, r^*)$ — measured: $\frac{Sgnl(k^*)}{Bckg(k^*)}$

$S(r^*)$ - emission function

$\Psi(k^*, r^*)$ - two-particle wave function (includes e.g. FSI interactions)

$\frac{Sgnl(k^*)}{Bckg(k^*)}$ - correlation function

Traditional and non-traditional femtoscopy

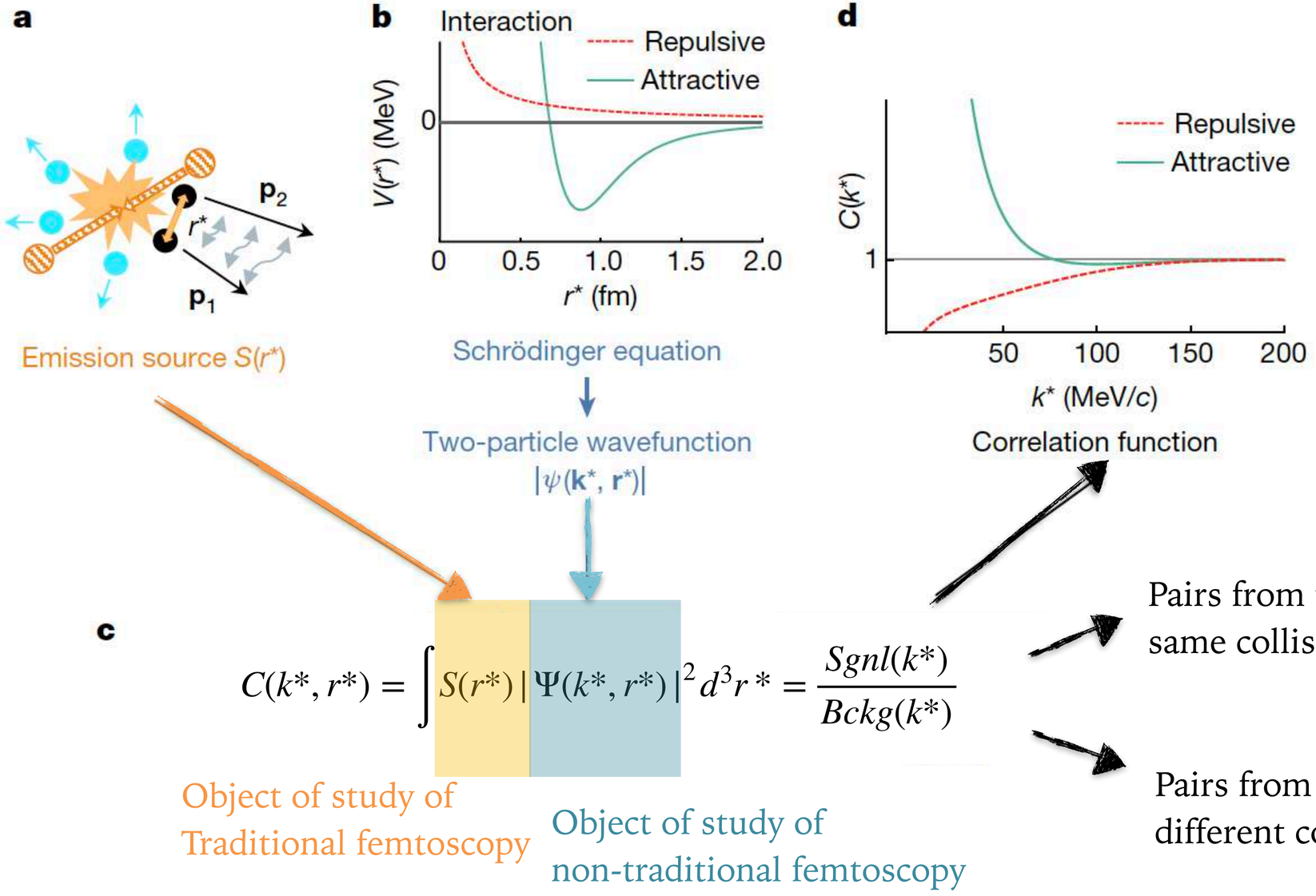

What does femtoscopy measure?

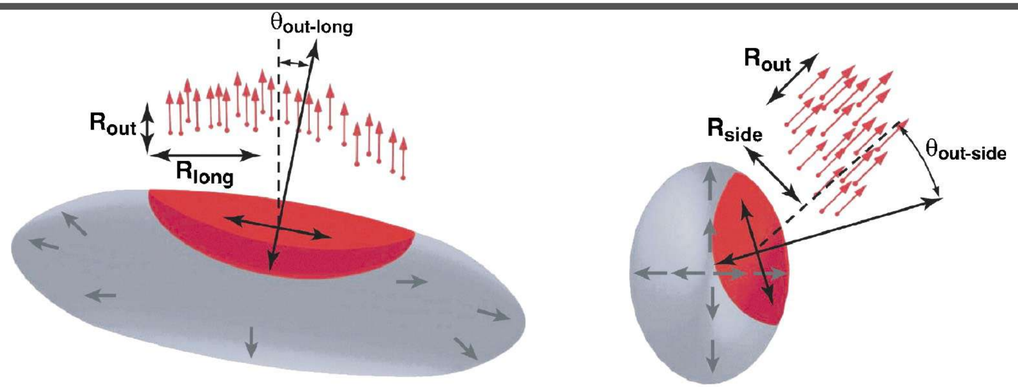

Lisa MA, et al. 2005.
Annu. Rev. Nucl. Part. Sci. 55:357–402

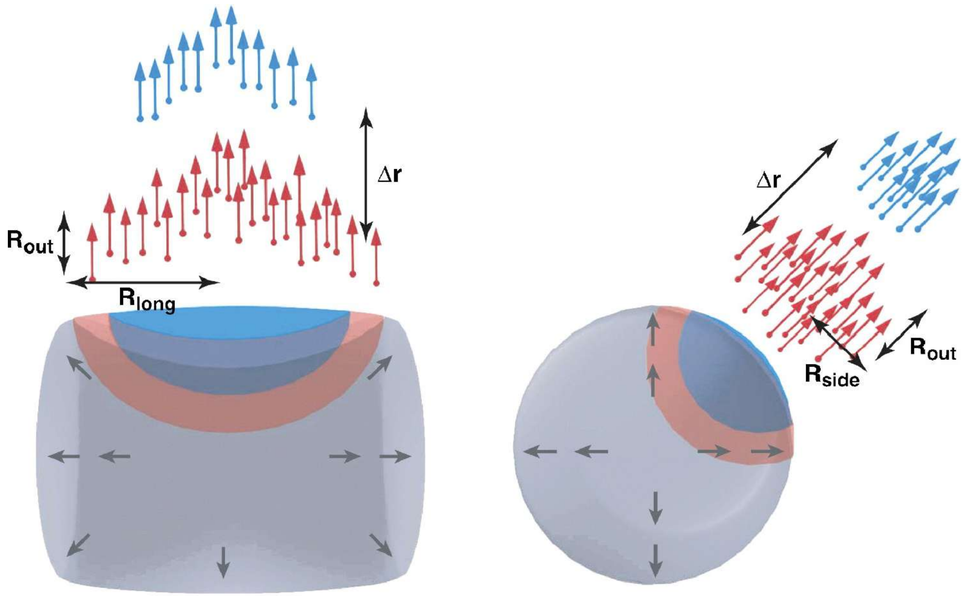

Lisa MA, et al. 2005.
Annu. Rev. Nucl. Part. Sci. 55:357–402

Homogeneity region

Q_{inv}

Longitudinal Co-Moving System - **LCMS**

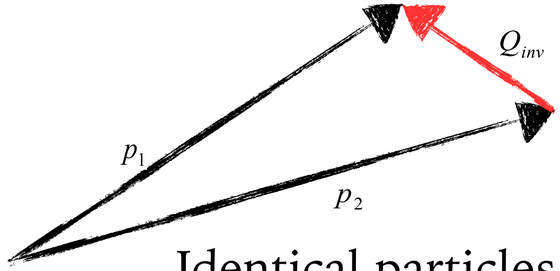

Identical particles

k^*

Pair Rest Frame - **PRF**

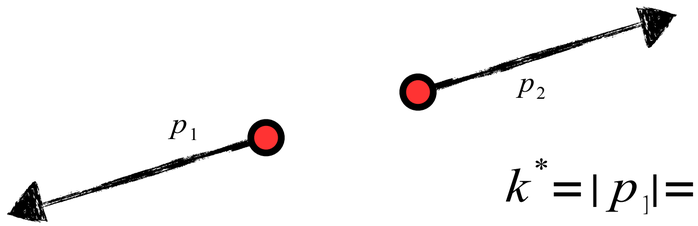

$k^* = |p_1| = |p_2|$

Nonidentical particles

$Q_{inv} = 2k^*$ for $m_1 = m_2$

Effects and interactions

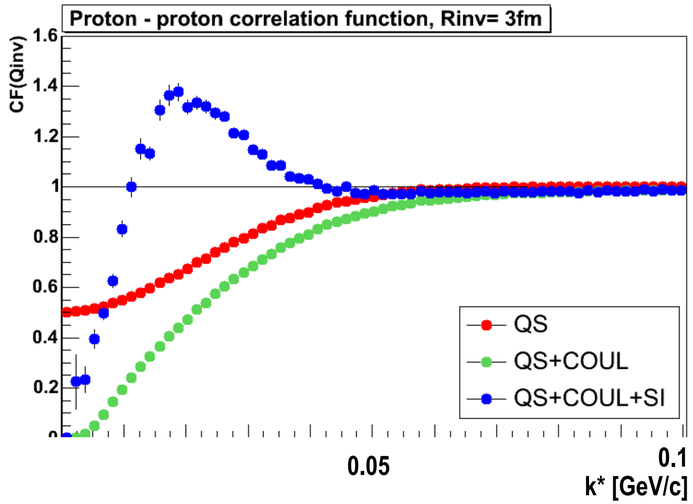

Identical baryon- baryon
- Quantum Statistics- **QS**
- Final State Interactions- **FSI**
  - Coulomb
  - Strong

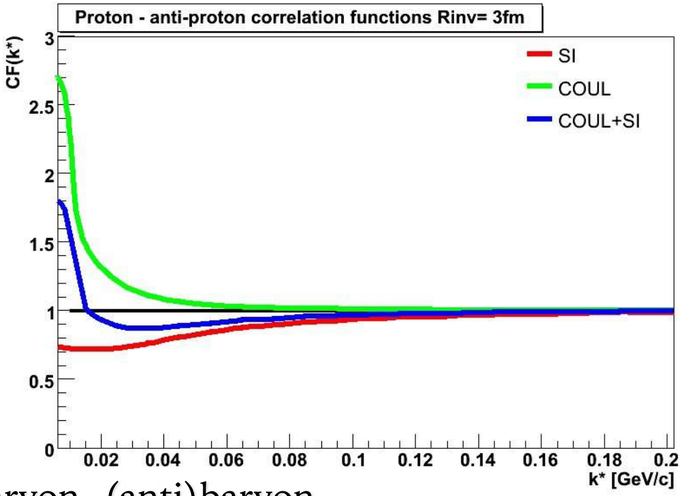

Non-identical baryon- (anti)baryon
- Final State Interactions- **FSI**
  - Coulomb
  - Strong

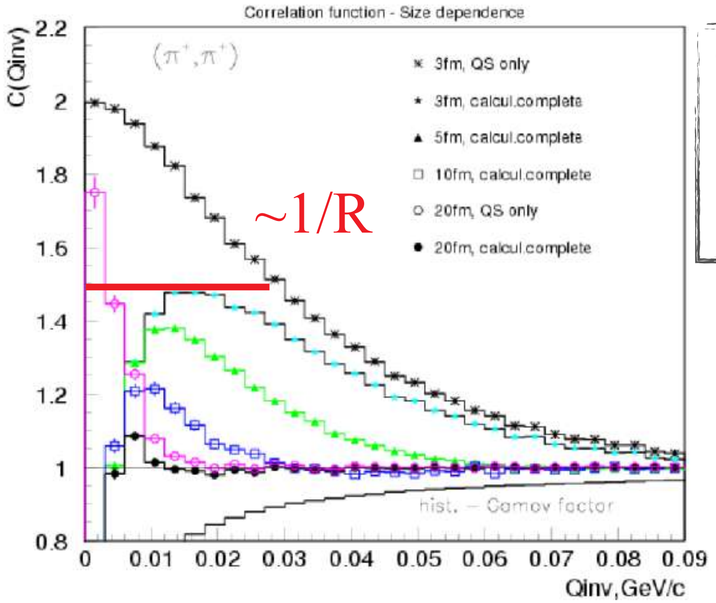

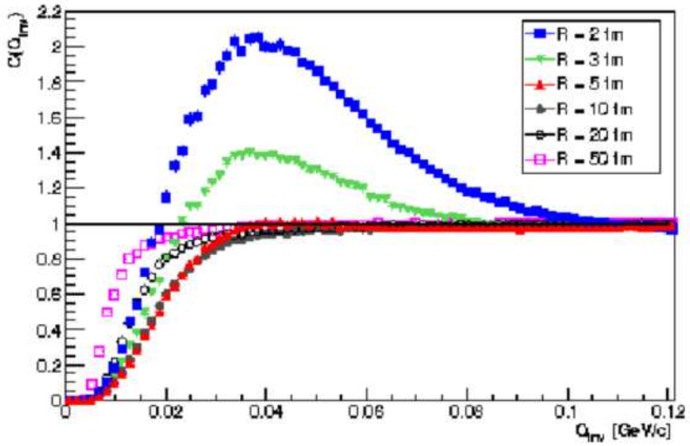

Width of
correlation function ~ **1/R**

Bigger source and
weaker correlation

Results

Published: 04 November 2015

Measurement of interaction between antiprotons

The STAR Collaboration

Nature **527**, 345–348 (2015) | Cite this article

This article has been updated

Abstract

One of the primary goals of nuclear physics is to understand the force between nucleons, which is a necessary step for understanding the structure of nuclei and how nuclei interact with each other. Rutherford discovered the atomic nucleus in 1911, and the large body of knowledge about the nuclear force that has since been acquired was derived from studies made on nucleons or nuclei. Although antinuclei up to antihelium-4 have been discovered[1] and their masses measured, little is known directly about the nuclear force between antinucleons. Here, we study antiproton pair correlations among data collected by the STAR experiment[2] at the Relativistic Heavy Ion Collider (RHIC)[3], where gold ions are collided with a centre-of-mass energy of 200 gigaelectronvolts per nucleon pair. Antiprotons are abundantly produced in such collisions, thus making it feasible to study details of the antiproton–antiproton interaction. By applying a technique similar to Hanbury Brown and Twiss intensity interferometry[4], we show that the force between two antiprotons is attractive. In addition, we report two key parameters that characterize the corresponding strong interaction: the scattering length and the effective range of the interaction. Our measured parameters are consistent within errors with the corresponding values for proton–proton interactions. Our results provide direct information on the interaction between two antiprotons, one of the simplest systems of antinucleons, and so are fundamental to understanding the structure of more-complex antinuclei and their properties.

Article | Open Access | Published: 09 December 2020

Unveiling the strong interaction among hadrons at the LHC

ALICE Collaboration

Nature **588**, 232–238 (2020) | Cite this article

A Publisher Correction to this article was published on 15 January 2021

This article has been updated

Abstract

One of the key challenges for nuclear physics today is to understand from first principles the effective interaction between hadrons with different quark content. First successes have been achieved using techniques that solve the dynamics of quarks and gluons on discrete space-time lattices[1,2]. Experimentally, the dynamics of the strong interaction have been studied by scattering hadrons off each other. Such scattering experiments are difficult or impossible for unstable hadrons[3,4,5,6] and so high-quality measurements exist only for hadrons containing up and down quarks[7]. Here we demonstrate that measuring correlations in the momentum space between hadron pairs[8,9,10,11,12] produced in ultrarelativistic proton–proton collisions at the CERN Large Hadron Collider (LHC) provides a precise method with which to obtain the missing information on the interaction dynamics between any pair of unstable hadrons. Specifically, we discuss the case of the interaction of baryons containing strange quarks (hyperons). We demonstrate how, using precision measurements of proton–omega baryon correlations, the effect of the strong interaction for this hadron–hadron pair can be studied with precision similar to, and compared with, predictions from lattice calculations[13,14]. The large number of hyperons identified in proton–proton collisions at the LHC, together with accurate modelling[15] of the small (approximately one femtometre) inter-particle distance and exact predictions for the correlation functions, enables a detailed determination of the short-range part of the nucleon-hyperon interaction.

QCD Phase diagram of strongly interacting matter

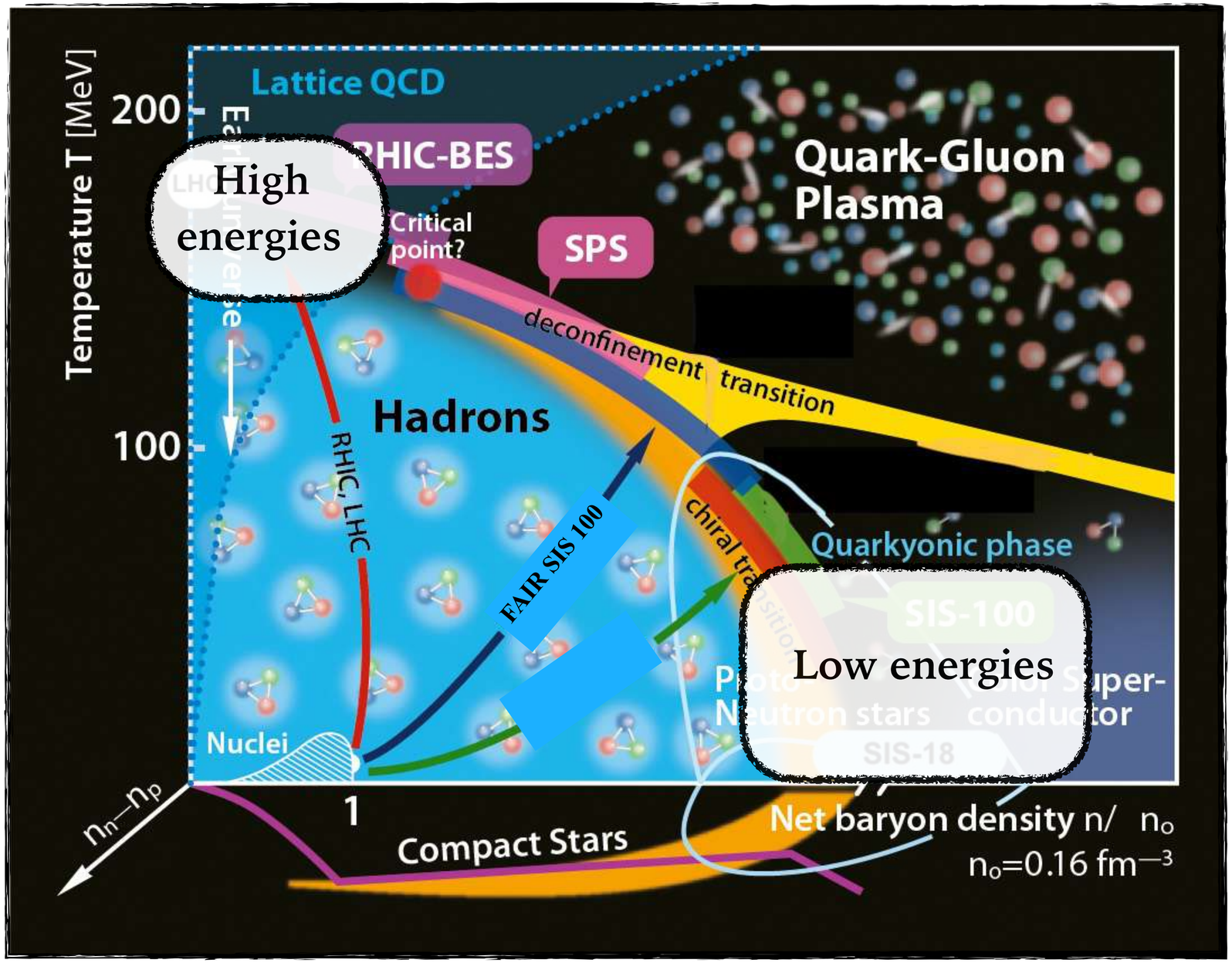

1a) Strong interactions between anti-nucleons

- The knowledge on **nuclear force** derived from studies of **nucleon** or / and **nuclei**.
- **Nuclear force** between **anti-nucleons** is studied for the first time.
- The knowledge of **interaction** between two **anti-protons** fundamental to understand the properties of more sophisticated anti-nuclei.

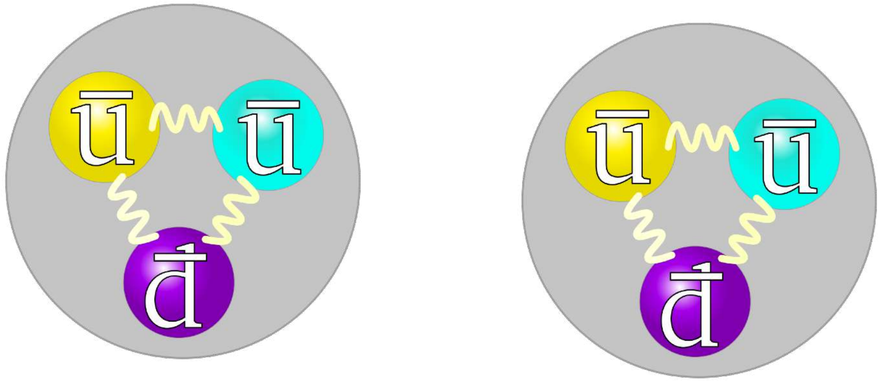

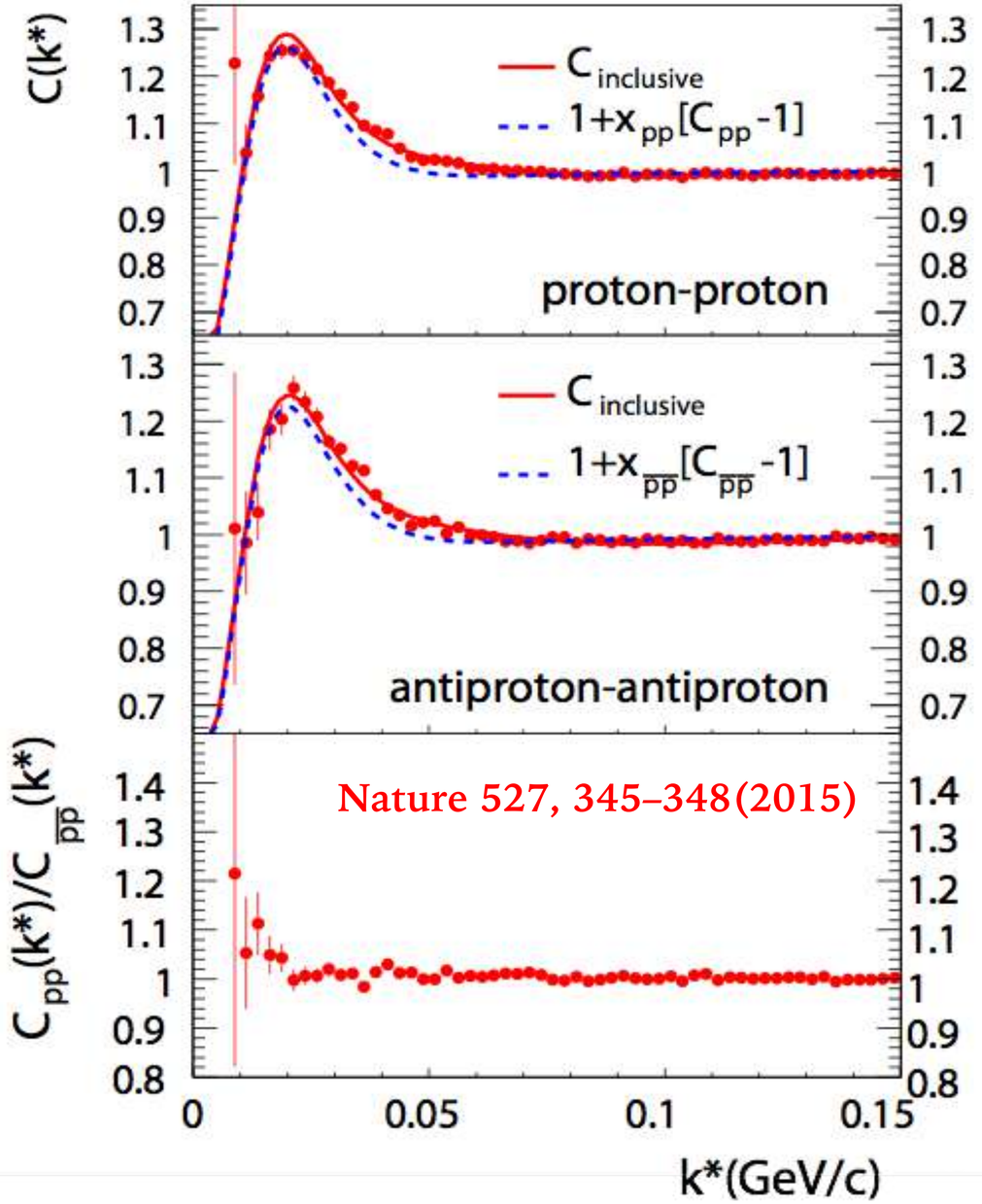

1a) Strong interactions between anti-nucleons

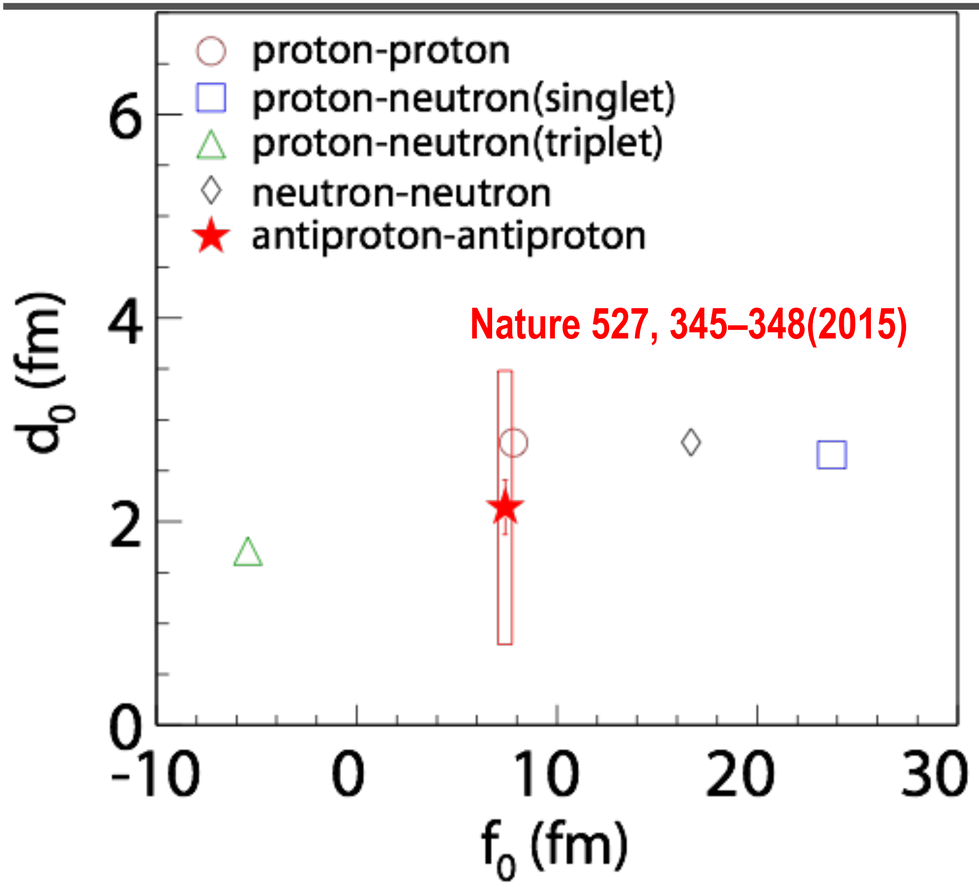

- f_0 and d_0 for the antiproton-antiproton interaction consistent with parameters for the proton-proton interaction.
- Descriptions of the interaction among antimatter (based on the simplest systems of anti-nucleons) determined.
- A quantitative verification of matter-antimatter symmetry in context of the forces responsible for the binding of (anti)nuclei.

The scattering length f_0: determines low-energy scattering.

The elastic cross section, σ_e, (at low energies) determined solely by the scattering length, $\lim_{k\to 0} \sigma_e = 4\pi f_0^2$

d_0 - the effective range of strong interaction between two particles.

It corresponds to the range of the potential in an extremely simplified scenario - the square well potential.

- f_0 and d_0 - two important parameters of strong interaction between two particles.
- Theoretical correlation function depends on: source size, k^*, f_0 and d_0.

1b) Inside a neutron star

Proceedings of the 12th Asia Pacific Physics Conference
JPS Conf. Proc. **1**, 011003 (2014)

Nuclear Matter in Neutron Stars –A Great Challenge in Nuclear Physics—

Hirokazu TAMURA[1]

[1]*Department of Physics, Tohoku University, Sendai 980-8578, Japan*

E-mail: tamura@lambda.phys.tohoku.ac.jp

(Received September 1, 2013)

Lack of our knowledge on the nuclear (hadronic) matter in the neutron star prevents us from understanding its internal structure. The elucidation of the neutron star matter is one of the most important and challenging subjects in nuclear physics today. The nuclear matter EOS (Equation Of State) which would describe pure neutron matter in the outer core of the neutron star is studied via various laboratory experiments particularly by using neutron-rich nuclei. Hyperons and/or kaons are expected to appear in the high density matter in the inner core, which is also experimentally investigated via hypernuclei and kaonic nuclei. Most of the EOS's including hyperons or kaons lead to a serious discrepancy against the large mass ($\sim 2M_{\odot}$) for the recently observed neutron stars, and resolution of this mystery requires new theoretical frameworks in nuclear physics which correctly describe high density matter, some of which may incorporate hadronic degrees of freedom with a deconfined quark matter phase.

1b) Neutron star puzzle

- **Hyperons**: expected in the core of neutron stars; **conversion of N into Y energetically favorable.**

- Appearance of Y: The relieve of Fermi pressure → **softer EoS** → **mass reduction (incompatible with observation)**

$M_{NS} \approx 1 \div 2\ M_\odot$

$R \approx 10\text{-}12$ km

$\rho \approx 3 \div 5\ \rho_0$

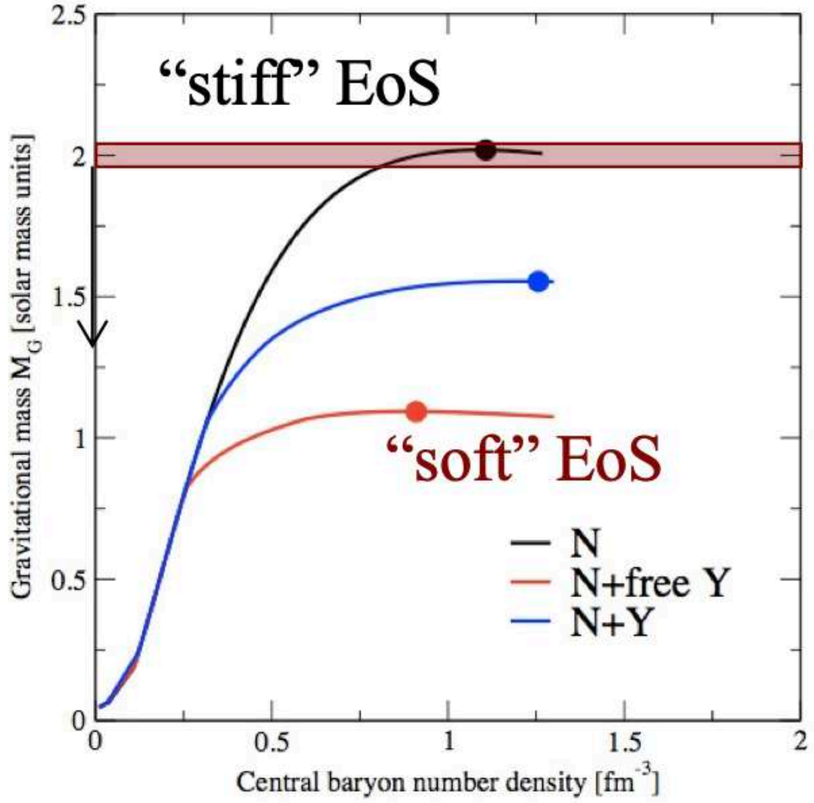

$\rho_0 \approx 2.8 \times 10^{14}$ g/cm^3

1b) Neutron star puzzle

- **Hyperons**: expected in the core of neutron stars; **conversion of N into Y energetically favorable.**

- Appearance of Y: The relieve of Fermi pressure → **softer EoS** → **mass reduction (incompatible with observation).**

$M_{NS} \approx 1 \div 2\ M_\odot$
$R \approx 10\text{-}12$ km
$\rho \approx 3 \div 5\ \rho_0$

The solution: a mechanism providing the **additional pressure** to make the EoS stiffer.

Possible mechanisms:

- **Two-body YN & YY interactions**
- Chiral forces
- Hyperonic Three Body Forces
- Quark Matter Core - Phase transition at densities lower than hyperon threshold

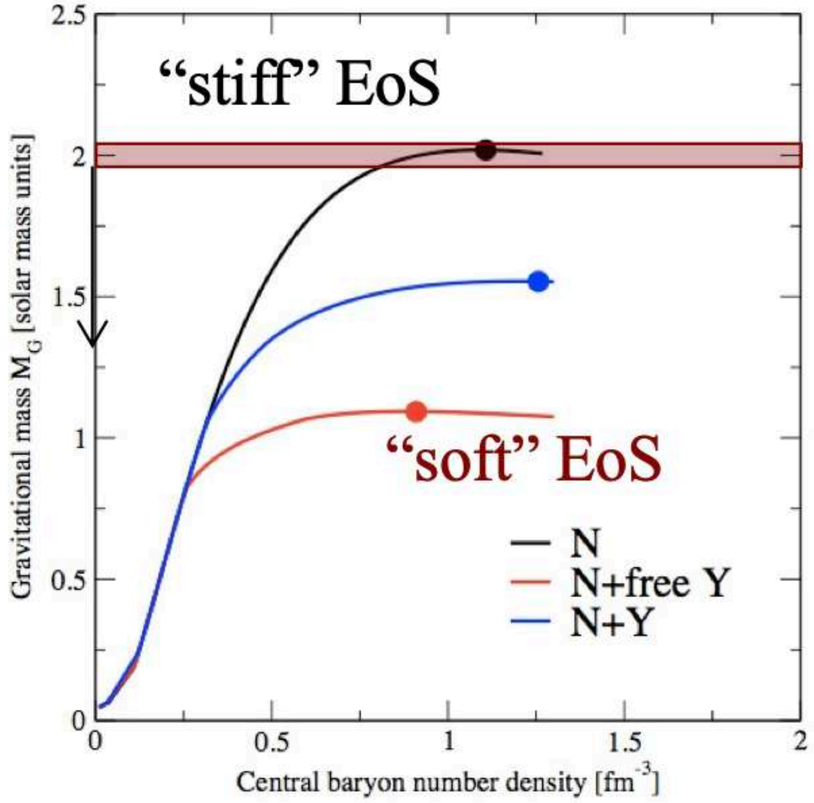

$\rho_0 \approx 2.8 \times 10^{14}$ g/cm^3

1b) Neutron star puzzle

- **Hyperons**: expected in the core of neutron stars; **conversion of N into Y energetically favorable.**

- Appearance of Y: The relieve of Fermi pressure → **softer EoS → mass reduction (incompatible with observation).**

$M_{NS} \approx 1 \div 2\ M_\odot$
$R \approx 10\text{-}12$ km
$\rho \approx 3 \div 5\ \rho_0$

The solution requires a mechanism that could provide the **additional pressure** at high densities needed to make the EoS stiffer.

Possible mechanisms:

- **Two-body YN & YY interactions**
- Chiral forces
- Hyperonic Three Body Forces
- Quark Matter Core - Phase transition at densities lower than hyperon threshold

A lot of experimental and theoretical effort to understand:

- The **KN** interaction, governed by the presence of **Λ(1405)**
- The nature of **Λ(1405)**, the consequences of **KNN** formation
- **K** and $\bar{K}$ investigated to understand kaon condensation

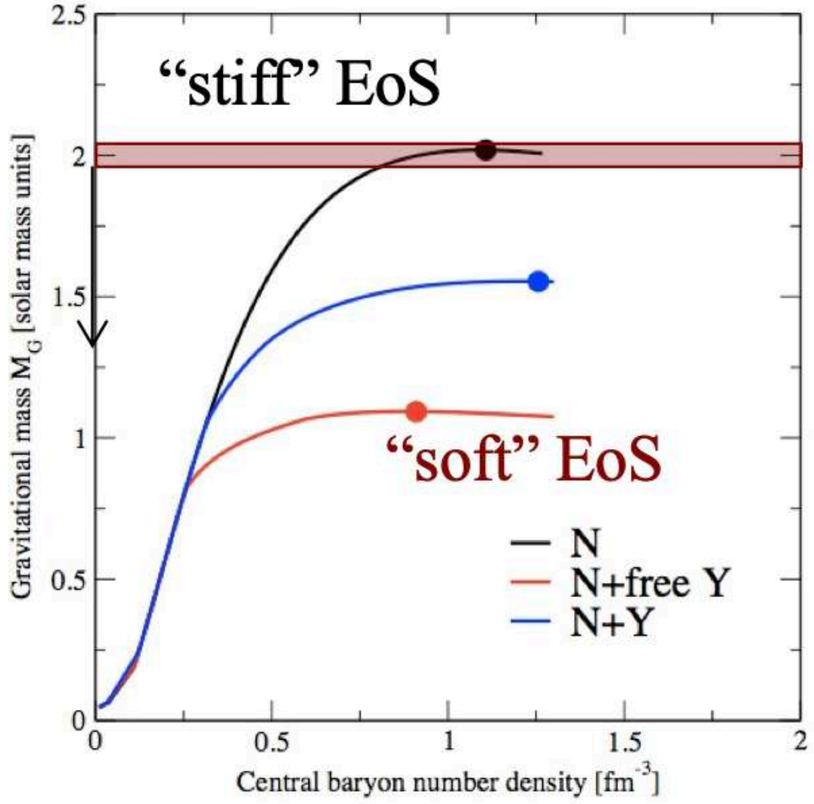

$\rho_0 \approx 2.8 \times 10^{14}$ g/cm^3

1b) Equation Of States for different types of baryonic matter

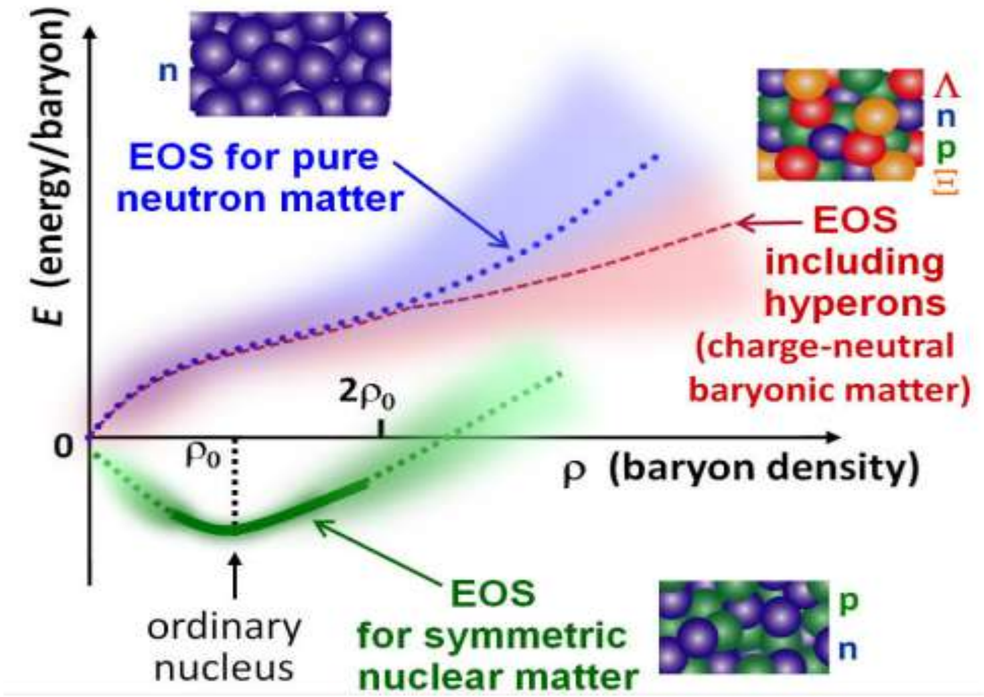

Fig. 1. A schematic illustration for nuclear (baryonic) matter Equation Of State (EOS) as a function of baryon density for symmetric nuclear matter, pure neutron matter, and charge-neutral baryonic matter with hyperons. The EOS is determined only for symmetric nuclear matter around $\rho \sim (0.5–2)\rho_0$ and has large uncertainties particularly for pure neutron matter, as symbolically shown in the figure.

„To establish the EOS applicable to the neutron star has been one of the most important subjects in nuclear physics for a long time but has not been achieved yet.”

H.Tamura, JPS Conf. Proc. , 011003 (2014)

1b) Equation Of States for different types of baryonic matter

Determining the Equation of State (EOS) of dense neutron-rich nuclear matter is a shared goal of both nuclear physics and astrophysics. Except possible phase transitions, the density dependence of **nuclear symmetry Esym(ρ) is the most uncertain part of the EOS of neutron-rich nucleonic matter especially at supra-saturation densities.**

„The Energy per nucleon **E(ρ, δ)** in nuclear matter at d**ensity ρ** and **isospin asymmetry** $\delta = (\rho_n - \rho_p)/\rho$ is the most basic input for calculating the EOS of neutron star matter regardless of the models used."

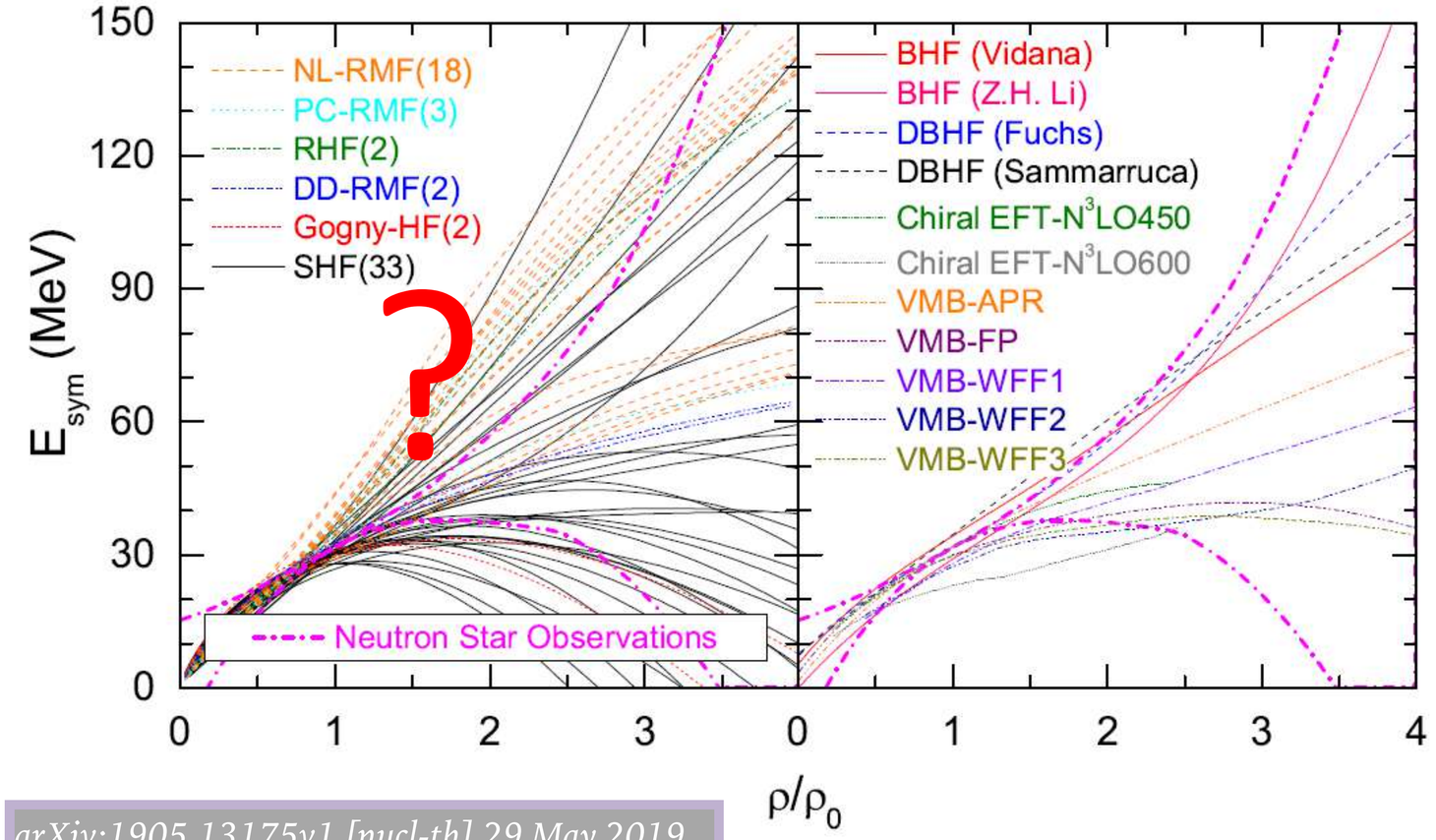

arXiv:1905.13175v1 [nucl-th] 29 May 2019

1b) Y-N and Y-Y interactions

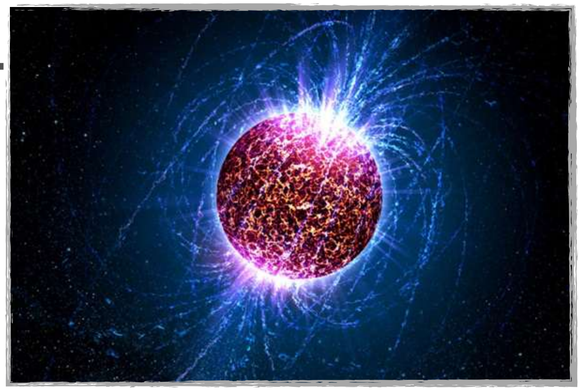

- **Experiment**: More interest about Y–N and Y–Y interactions.
- **Theory**: Major steps forward have been made (Lattice QCD).
- **Numerous theoretical predictions** exist, but no clear evidence for any such **bound states**, despite **many experimental searches**.
- The existence of **hypernuclei** (confirmed by attractive Y–N interaction) → indicates the possibility to bind Y to N.
- The measurement of the Y–N and Y–Y interactions leads to important implications for the possible formation of **Y–N** or **Y–Y bound states**.
- A precise knowledge of these interactions help to explore unknown structure of neutron stars.

1c) YN interactions at HADES

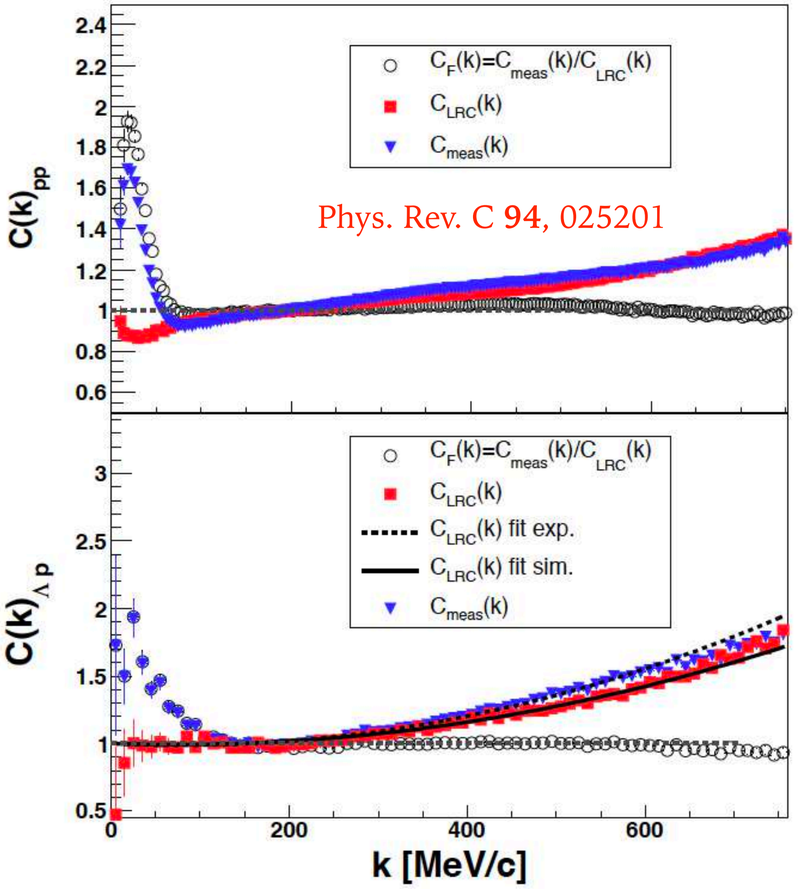

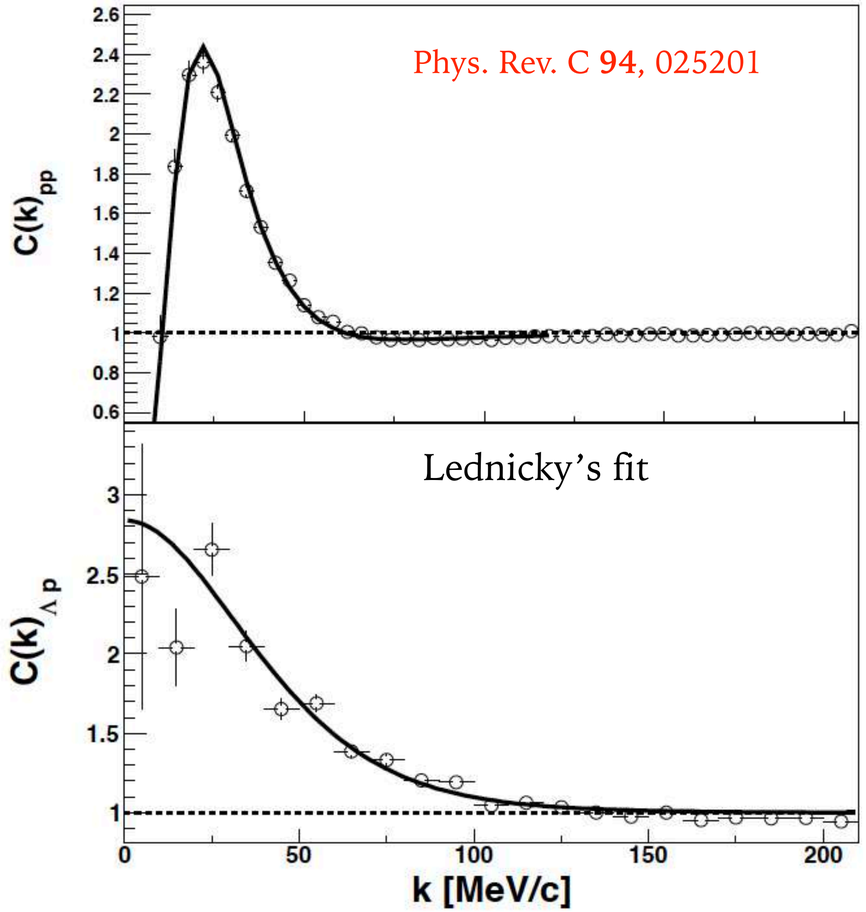

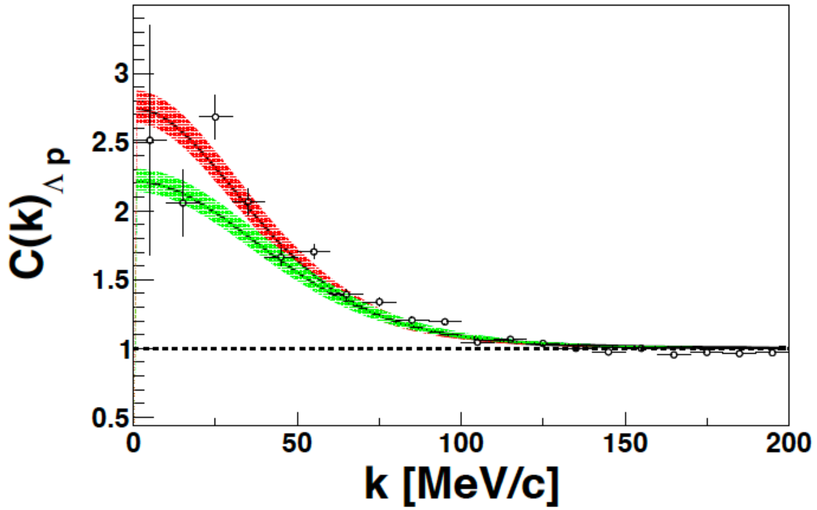

NLO scattering paremeters

$f_{0,NLO}^{S=0} = 2.91fm$

$d_{0,NLO}^{S=0} = 2.78fm$

$f_{0,NLO}^{S=1} = 1.54fm$

$d_{0,NLO}^{S=1} = 2.72fm$

LO scattering parameters

$f_{0,LO}^{S=0} = 1.91fm$

$d_{0,LO}^{S=0} = 1.40fm$

$f_{0,LO}^{S=1} = 1.23fm$

$d_{0,LO}^{S=1} = 2.13fm$

$$C_F(k) = \frac{C_{meas}(k)}{C_{LRC}(k)}$$

$$C_{LRC}(k^*) = 1 + ak + bk^2$$

The femtoscopy technique to study **interactions** between particles can be applied to many colliding systems at very **different energies**, which can help to improve the understanding of H-Y interactions.

1c) Strange Baryon Correlations (Including Λ Hyperons)

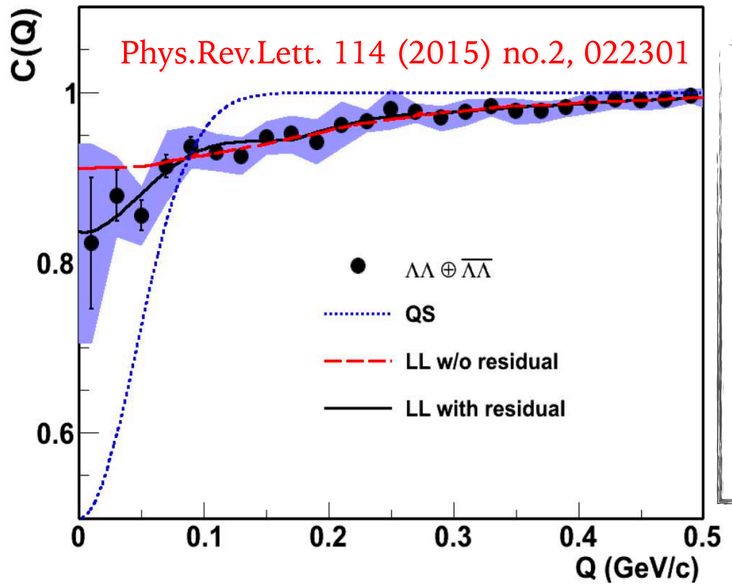

- The binding energy of $\Lambda - \Lambda$ **bound state** estimated within an effective-range expansion approach.
- Search go **H-dibaryon** not completed.

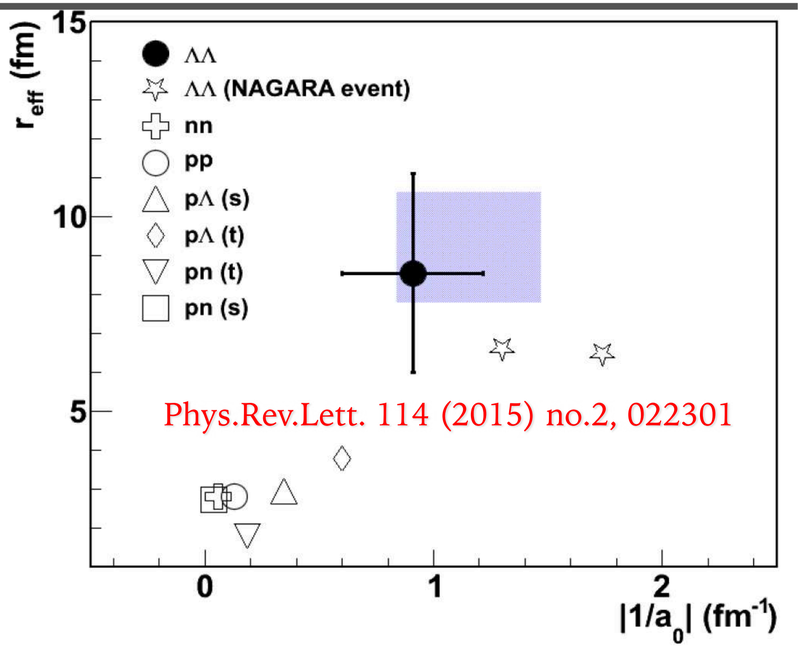

N	lambda	r0	1/f0	d0	ares	rres
1.0	0.5	2.0 fm	1.0 fm	3.0 fm	-0.04	0.05 fm

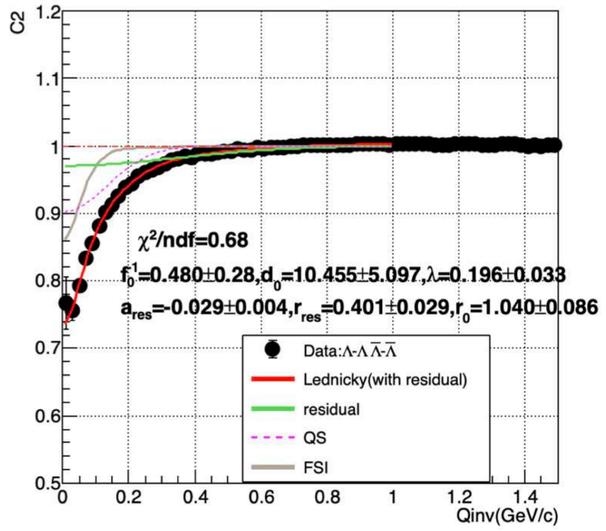

F0 became positive!!

1/f0	0.480fm
d0	10.455fm

ALICE's study

ALICE Collaboration Phys. Lett. B 797 (2019) 134822

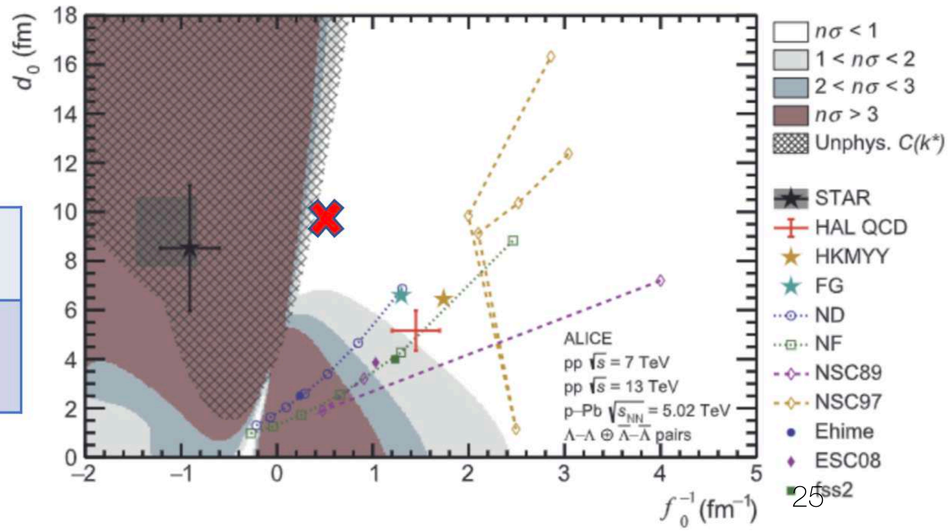

1d) Strange Baryon Correlations (including p-Ω)

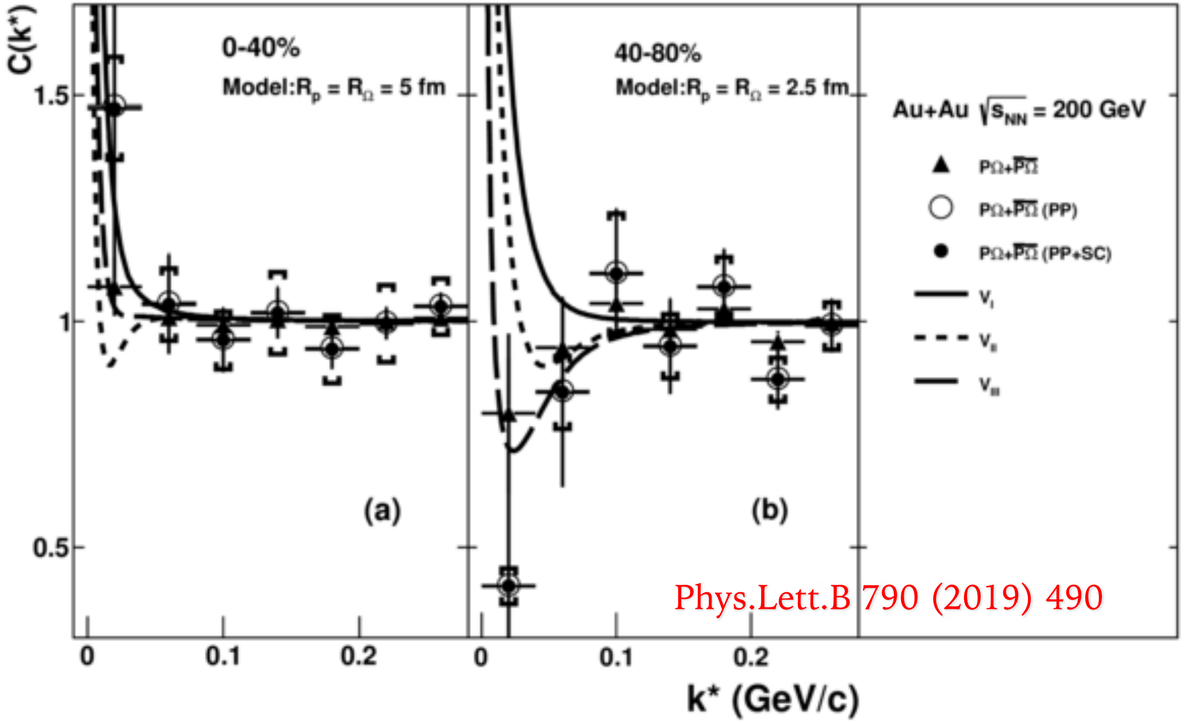

Phys.Lett.B 790 (2019) 490

Scattering lenght positive, **favor the hypothesis of pΩ bound state**

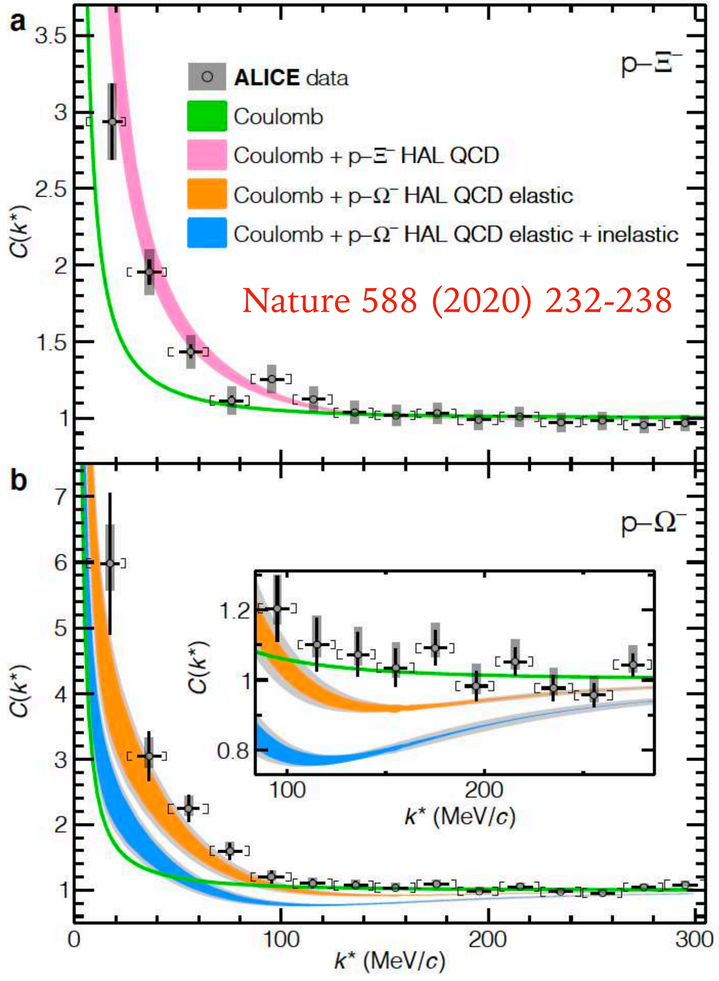

Nature 588 (2020) 232-238

	V_1	V_2	V_3
E_{bin} [MeV]	-	6.3	26.9
a_0 [MeV]	-1.12	5.79	1.29
r_{eff} [MeV]	-1.16	0.96	0.65

1d) Strange Baryon Correlations (Including Ξ Hyperons)

First measurement of Ξ-Ξ correlation at RHIC

Combination of **quantum statistics**, **strong** interaction, and **Coulomb** interaction.

Anti-correlation at Q < 0.25 GeV/c.

Lattice QCD/chiral EFT calculations indicate an attractive interaction potential, but not strong enough to form a bound state.

N	lambda	r0	1/f0	d0
1.0	0.5	1.5fm	1.0 fm	5.0 fm

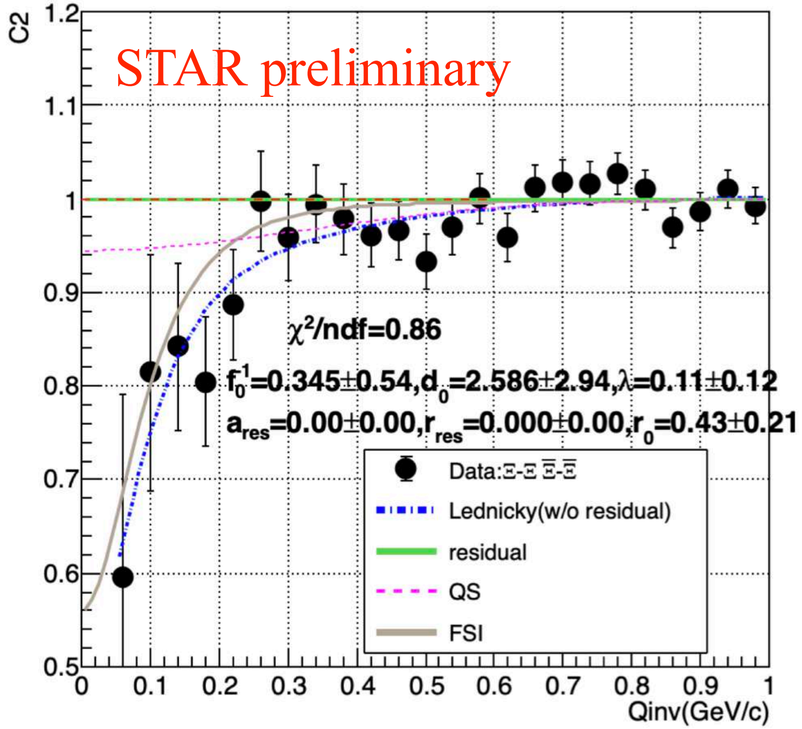

F0 became positive!!

1/f0	0.345fm
d0	2.586fm

1d) Proton-kaon (bound state?)

Same charges 0-10% @ Au+Au 39 GeV

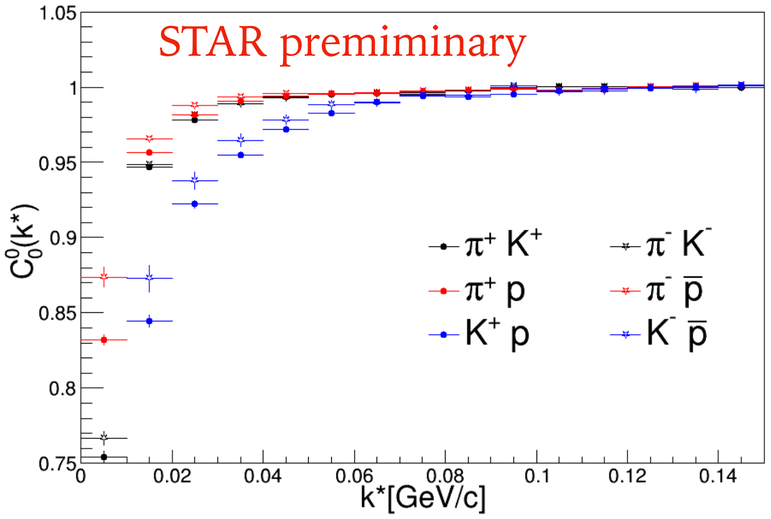

Opposite charges 0-10% @ Au+Au 39 GeV

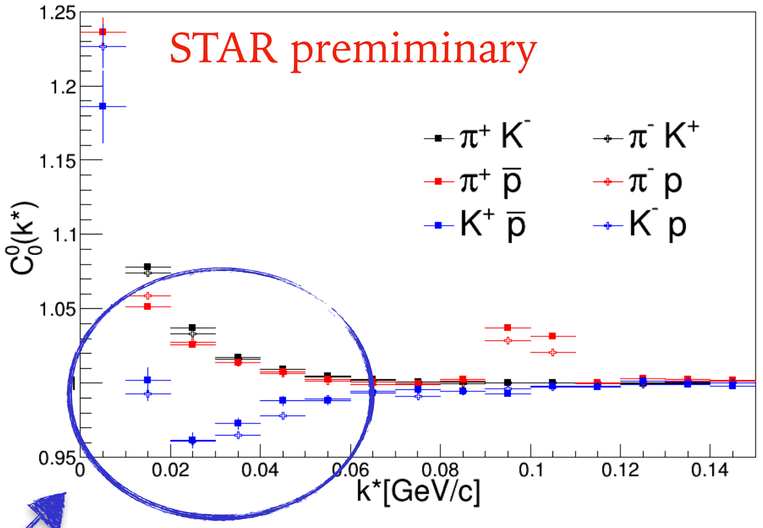

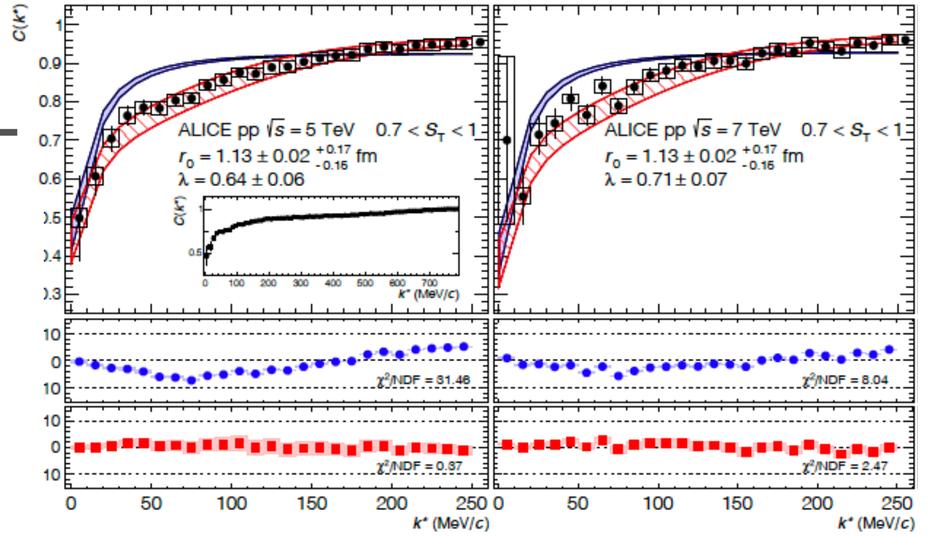

Phys.Lett.B 813 (2021) 136030

- High-precision measurement of the **strong interaction (anti-correlation)** between kaons and protons.
- A structure (ALICE in p+p collisions) observed around a relative momentum of 58 MeV/c in the measured correlation function of opposite charges in p+p collisions.

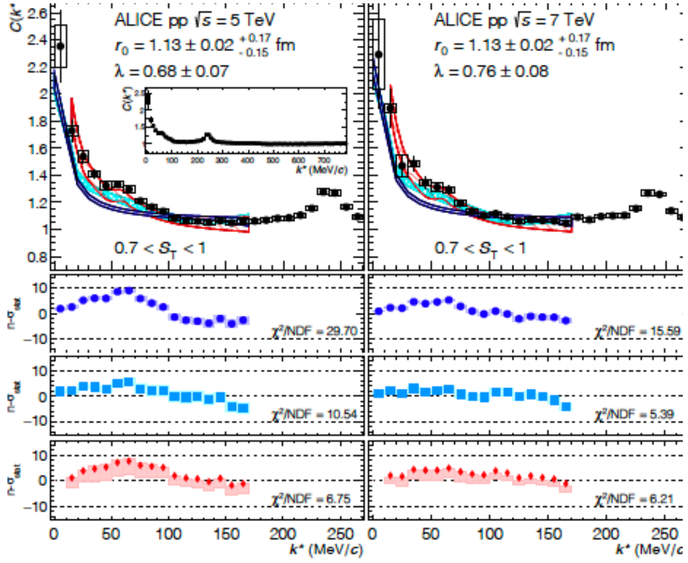

1d) Neutral kaons

Parametrization - $K_s^0 K_s^0$

Gaussian density distribution (includes only **QS effects**): $CF(q_{inv}) = 1 + \lambda e^{[-R_{inv}^2 q_{inv}^2]}$

λ - the correlation strength, R_{inv} - the size of the particle-emitting source.

Lednicky & Lyuboshitz model includes **strong FSI**: [Sov.J.Nucl.Phys. 35, 770 (1982)]

$$CF(q_{inv}) = 1 + \lambda\left(e^{[-R_{inv}^2 q_{inv}^2]} + \frac{1}{2}\left[\left|\frac{f(k^*)}{R_{inv}}\right|^2 + \frac{4\Re f(k^*)}{\sqrt{\pi}R_{inv}} F_1(q_{inv}R_{inv}) - \frac{2\Im f(k^*)}{\sqrt{\pi}R_{inv}} F_2(q_{inv}R_{inv})\right]\right)$$

QS effect

strong FSI through the $f_0(980)$ and $a_0(980)$ resonances

$$F_1(z) = \int_0^z dx \frac{e^{x^2} - x^2}{z},\ F_2(z) = \frac{1 - e^{x^2}}{z}$$

$$f(k^*) = \frac{1}{2}[f_0(k^*) + f_1(k^*)],\quad f_I(k^*) = \frac{\gamma_r}{m_r - s - i\gamma_r k^* - i\gamma_r' k_r'},\quad s = 4\left(m_K^2 + k^{*2}\right)$$

	$m_{f_0}\left[\frac{GeV}{c^2}\right]$	$\gamma_{f_0 K\bar{K}}$	$\gamma_{f_0\pi\pi}$	$m_{a_0}\left[\frac{GeV}{c^2}\right]$	$\gamma_{a_0 K\bar{K}}$	$\gamma_{a_0\pi\pi}$
Antonelli [1]	0.973	2.763	0.5283	0.985	0.4038	0.3711
Achasov2001 [2]	0.996	1.305	0.2684	0.992	0.5555	0.4401
Achasov2003 [3]	0.996	1.305	0.2684	1.003	0.8365	0.4580
Martin [4]	0.978	0.792	0.1990	0.974	0.3330	0.2220

[1] eConf C020620, THAT06 (2002), [2] Phys. Rev. D 63, 094007 (2001)
[3] Phys. Rev. D 68, 014006 (2003), [4] Nucl. Phys. B 121, 514–530 (1977)

1d) Neutral kaons

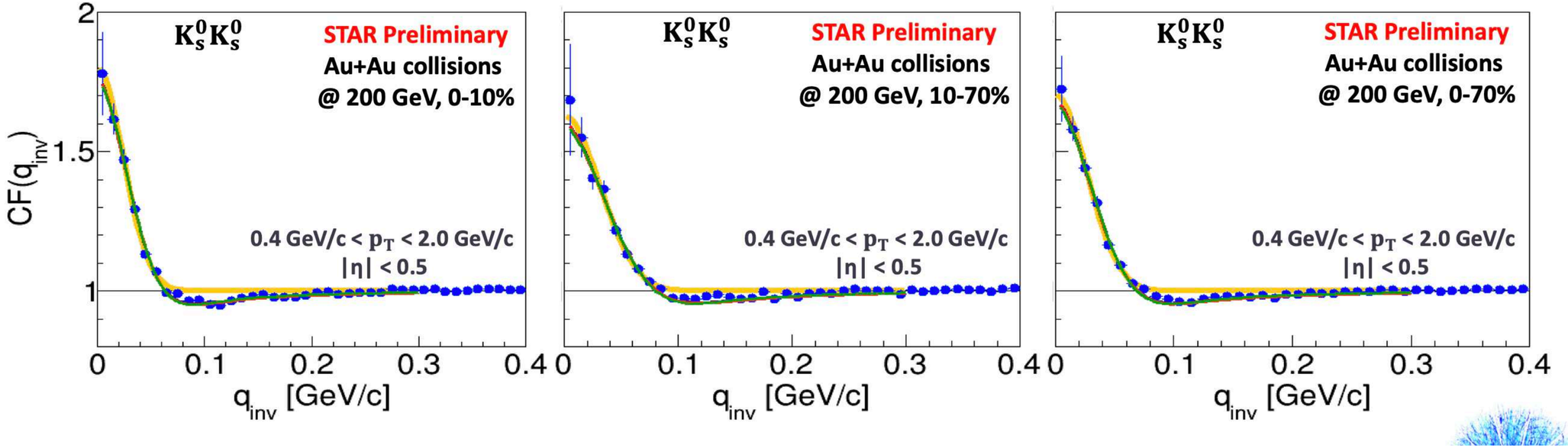

The **strong** final-state interaction has a significant effect on the **neutral kaons** correlation due to the near-threshold $f_0(980)$ **and** $a_0(980)$ resonances

1d) Neutral kaons

Parametrization - $K^0_S K^{\pm}$

Lednicky & Lyuboshitz model includes strong FSI: [Sov.J.Nucl.Phys. 35, 770 (1982)]

$$CF(k^*) = 1 + \frac{\lambda}{4}\left[\left|\frac{f(k^*)}{R}\right|^2 + \frac{4\Re f(k^*)}{\sqrt{\pi}R}F_1(2k^*R) - \frac{2\Im f(k^*)}{\sqrt{\pi}R}F_2(2k^*R)\right]$$

strong FSI through the $a_0(980)$ resonance

$$F_1(z) = \int_0^z dx \frac{e^{x^2}-x^2}{z},\ F_2(z) = \frac{1-e^{x^2}}{z}$$

$$f(k^*) = \frac{\gamma_r}{m_r - s - i\gamma_r k^* - i\gamma'_r k'_r},\qquad s = 4\left(m_K^2 + k^{*2}\right)$$

	$m_{a_0}\left[\frac{GeV}{c^2}\right]$	$\gamma_{a_0 K\bar{K}}$	$\gamma_{a_0 \pi\eta}$
Antonelli [1]	0.985	0.4038	0.3711
Achasov2001 [2]	0.992	0.5555	0.4401
Achasov2003 [3]	1.003	0.8365	0.4580
Martin [4]	0.974	0.3330	0.2220

[1] eConf C020620, THAT06 (2002), [2] Phys. Rev. D 63, 094007 (2001)
[3] Phys. Rev. D 68, 014006 (2003), [4] Nucl. Phys. B 121, 514–530 (1977)

1d) Neutral kaons

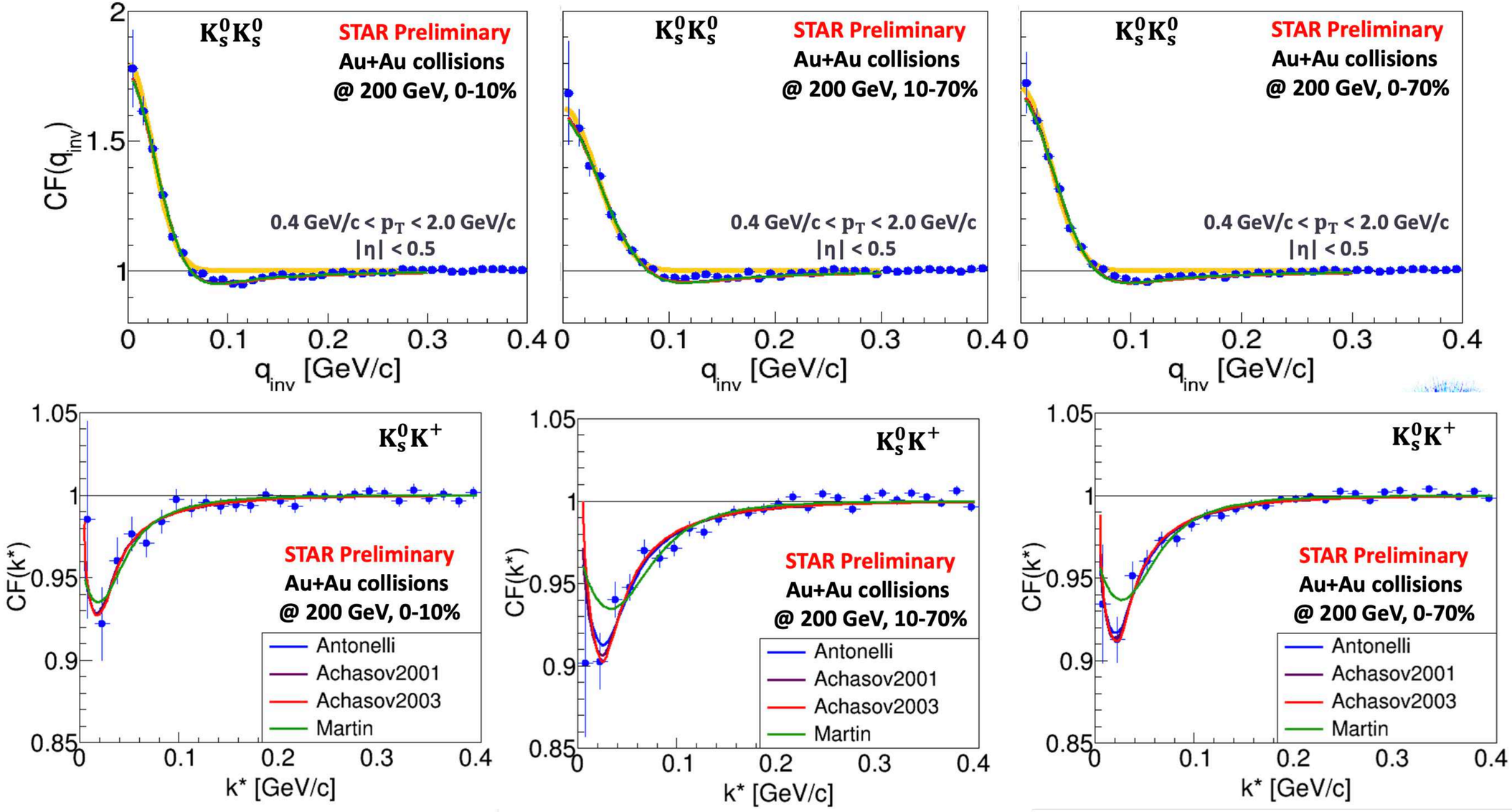

The $a_0(980)$ FSI parametrization gives very good representation of the shape of the signal region in CF; the parametrization with the larger $a_0(980)$ mass and decay coupling gives larger size of the source; **Antonelli parametrization favors $a_0(980)$ resonance as a tetraquark**

1d) Neutral kaons

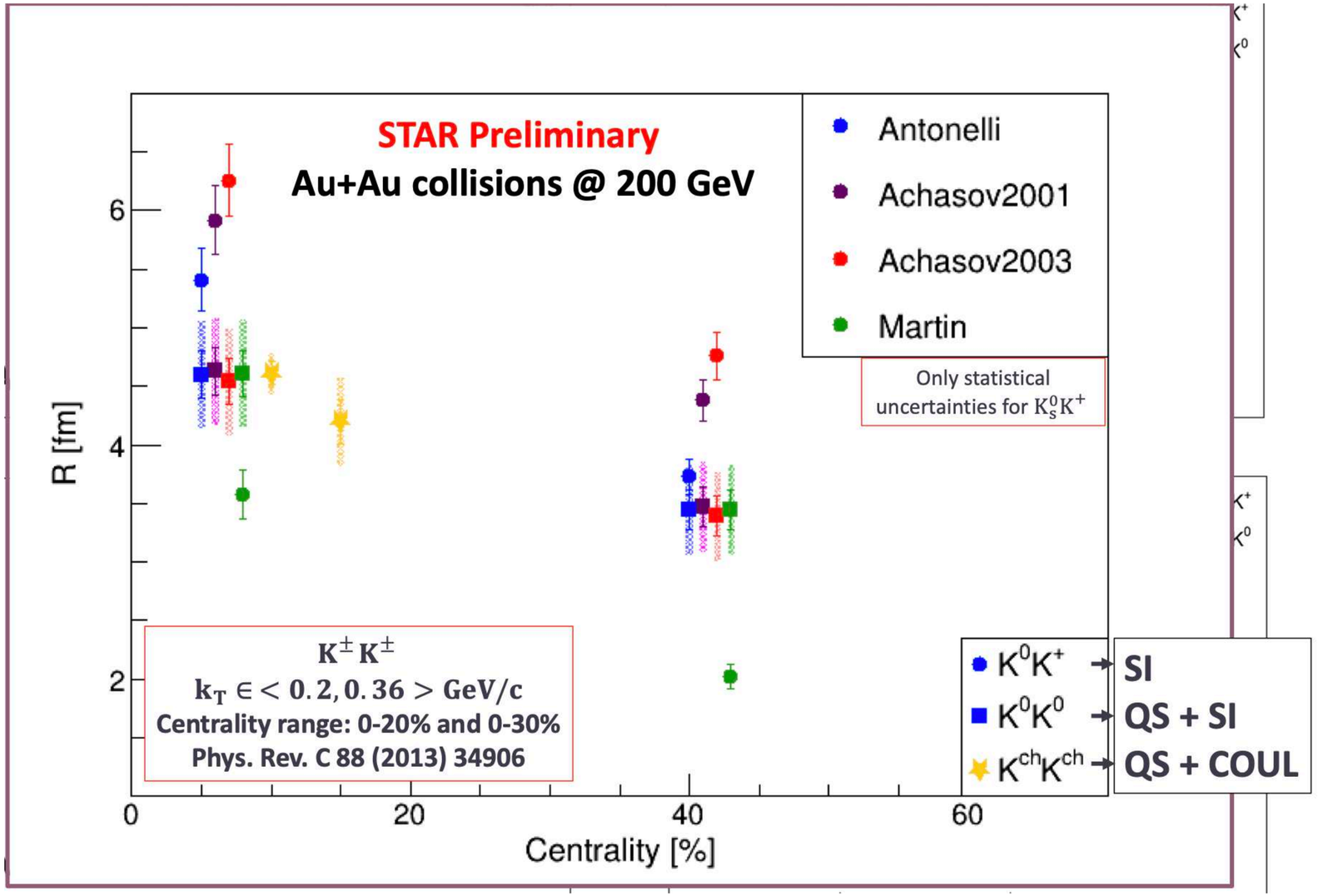

The $a_0(980)$ FSI parametrization gives very good representation of the shape of the signal region in CF; the parametrization with the larger $a_0(980)$ mass and decay coupling gives larger size of the source; **Antonelli parametrization favors $a_0(980)$ resonance as a tetraquark**

1e) Light nuclei formation at STAR

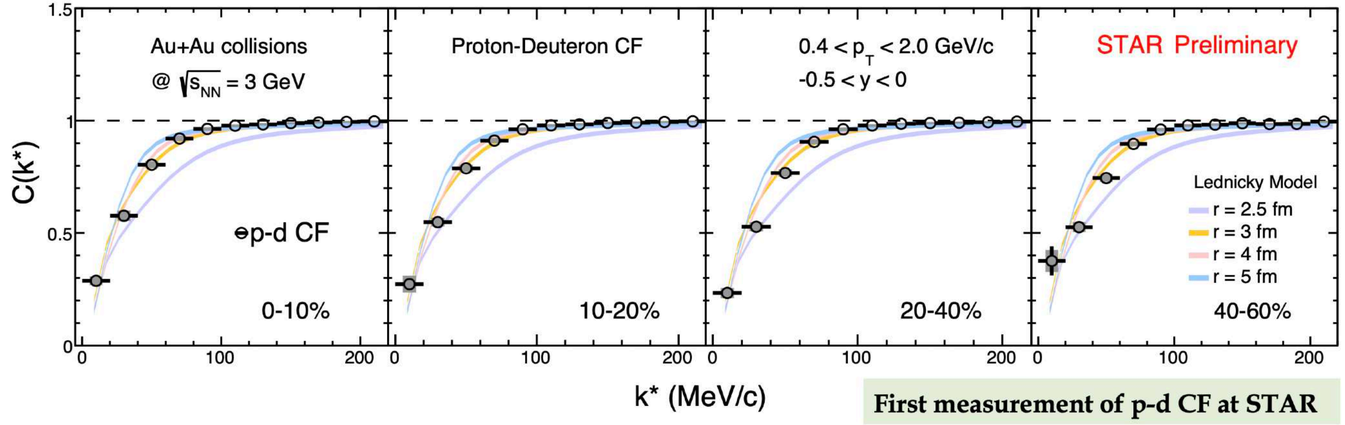

First measurement of p-d CF at STAR

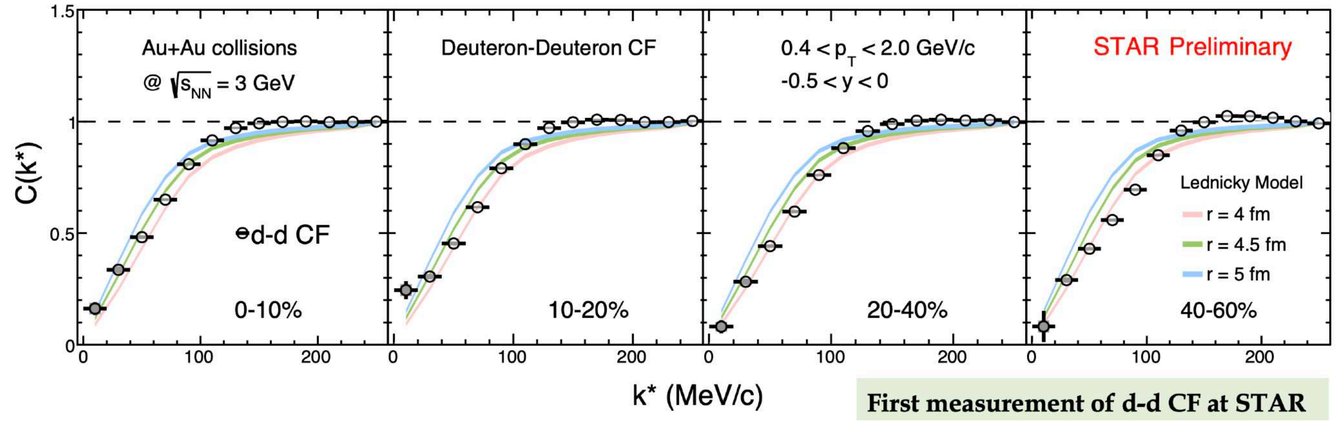

First measurement of d-d CF at STAR

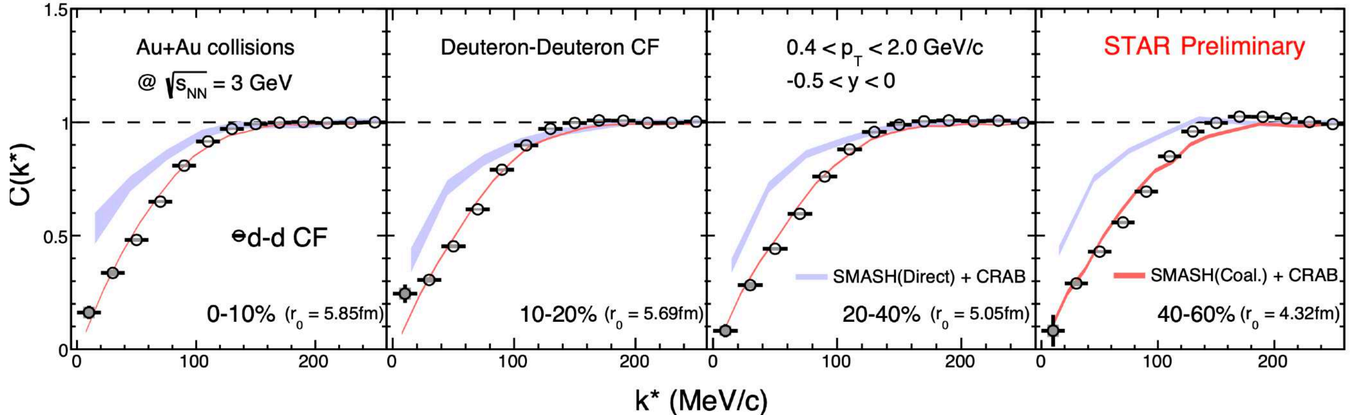

- First measurement of **proton-deuteron** and **deuteron-deuteron** correlation functions from STAR

- **Proton-deuteron** and **deuteron-deuteron** correlations qualitatively described by the Lednicky-Lyuboshits model; deuteron-deuteron has larger emission source size than proton-deuteron

- Deuteron-deuteron correlations described better by the model including **coalescence**. Light nuclei are likely to be formed via coalescence.

1f) Kaon-Lambda

To measure scattering parameters of $\Lambda - K$ pairs in all three charge combinations $\Lambda - K^+$, $\Lambda - K^-$ and $\Lambda - K^0_S$.

Strong force is **repulsive** in the $\Lambda - K^+$ interaction and **attractive** in the $\Lambda - K^-$ and $\Lambda - K^0_S$ interactions.

Different $q - \bar{q}$ interactions between the pairs ($s - \bar{s}$ in $\Lambda - K^+$ and $\Lambda - K^0_S$ and $u - \bar{u}$ in $\Lambda - K^-$)

Different net-strangeness for each system (S=0 for $\Lambda - K^+$, and S=-2 for $\Lambda - K^-$).

Source radii larger than expected from extrapolation from identical particle femtoscopic studies, due to separation in space–time of the single-particle Λ and K source distributions.

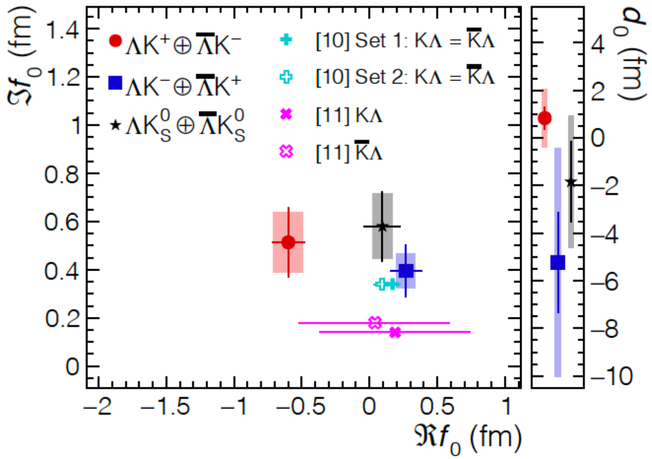

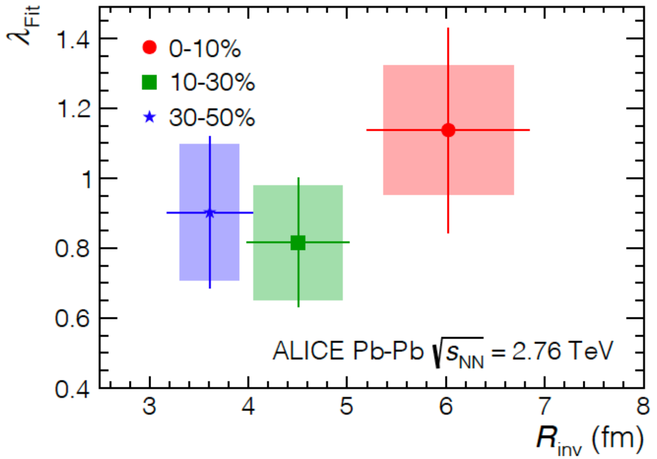

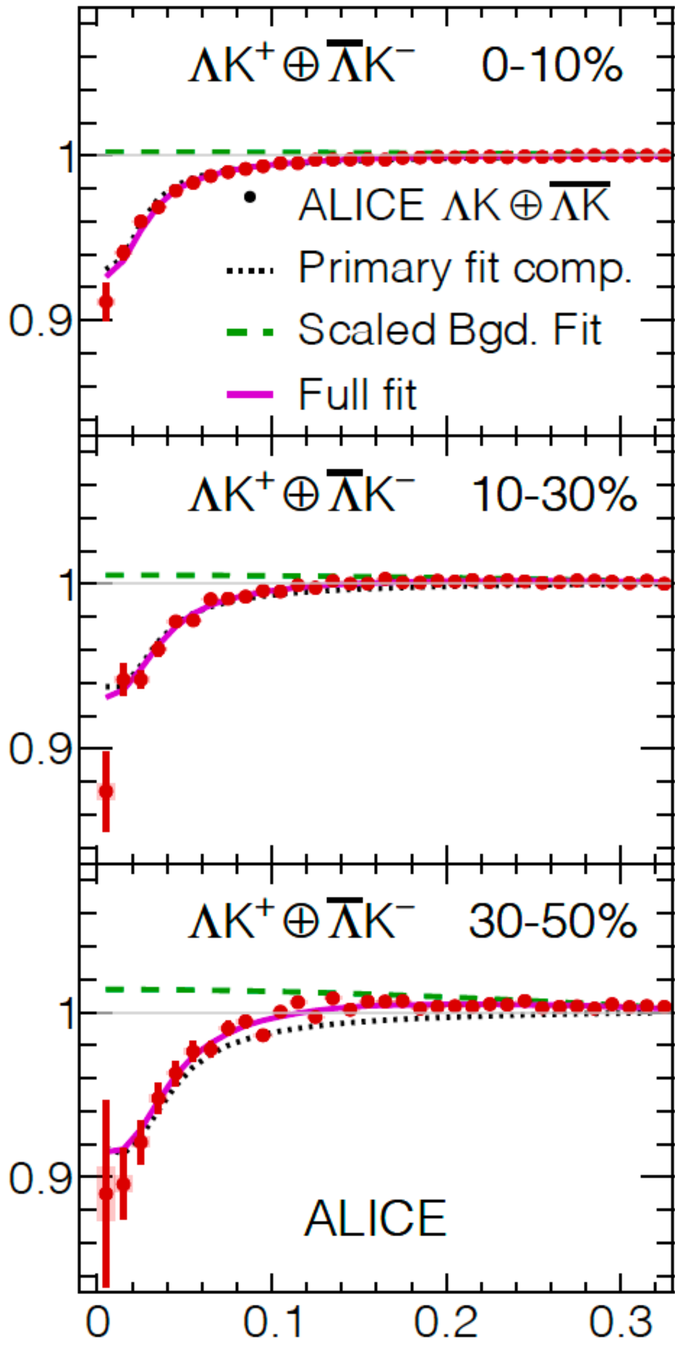

CBM (and HADES) challenges

Challenges in QCD matter physics – The scientific programme of the Compressed Baryonic Matter experiment at FAIR

diagnostic probes which are sensitive to the dense phase of the nuclear fireball. The goal of the CBM experiment at SIS100 ($\sqrt{s_{NN}} = 2.7 - 4.9$ GeV) is to discover fundamental properties of QCD matter: the phase structure at large baryon-chemical potentials ($\mu_B > 500$ MeV), effects of chiral symmetry, and the equation-of-state at high density as it is expected to occur in the core of neutron stars. In this article, we review the motivation for and the physics programme of CBM, including activities before the start of data taking in 2024, in the context of the worldwide efforts to explore high-density QCD matter.

arXiv:1607.01487v3 [nucl-ex] 29 Mar 2017

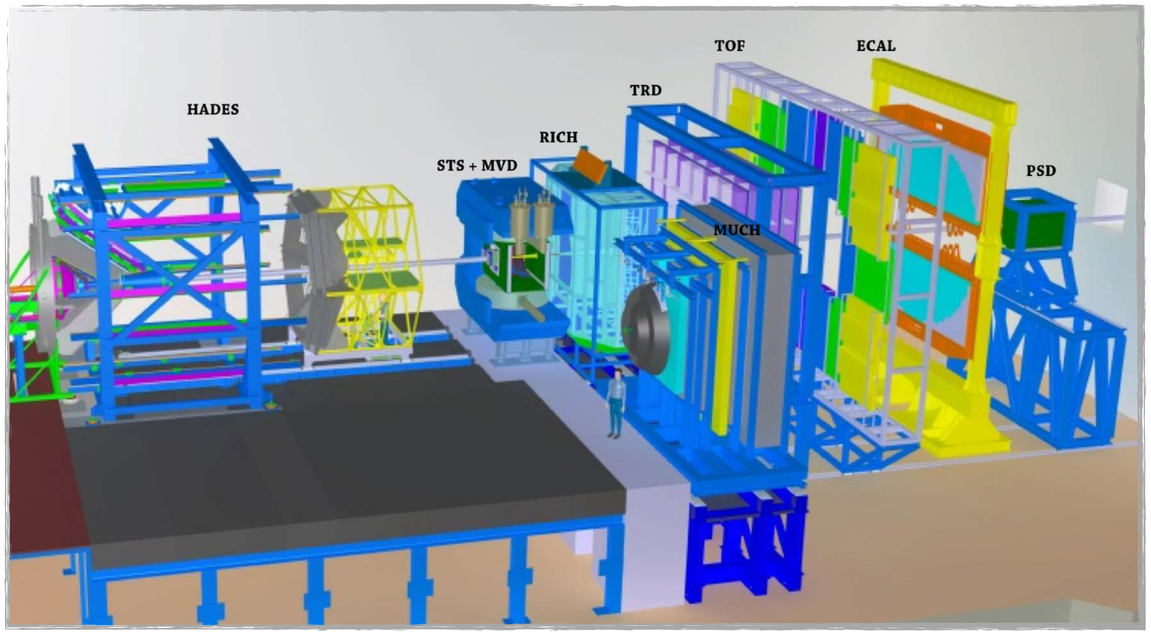

The CBM experimental setup together with the HADES detector

QCD Phase diagram of strongly interacting matter - intermediate energies

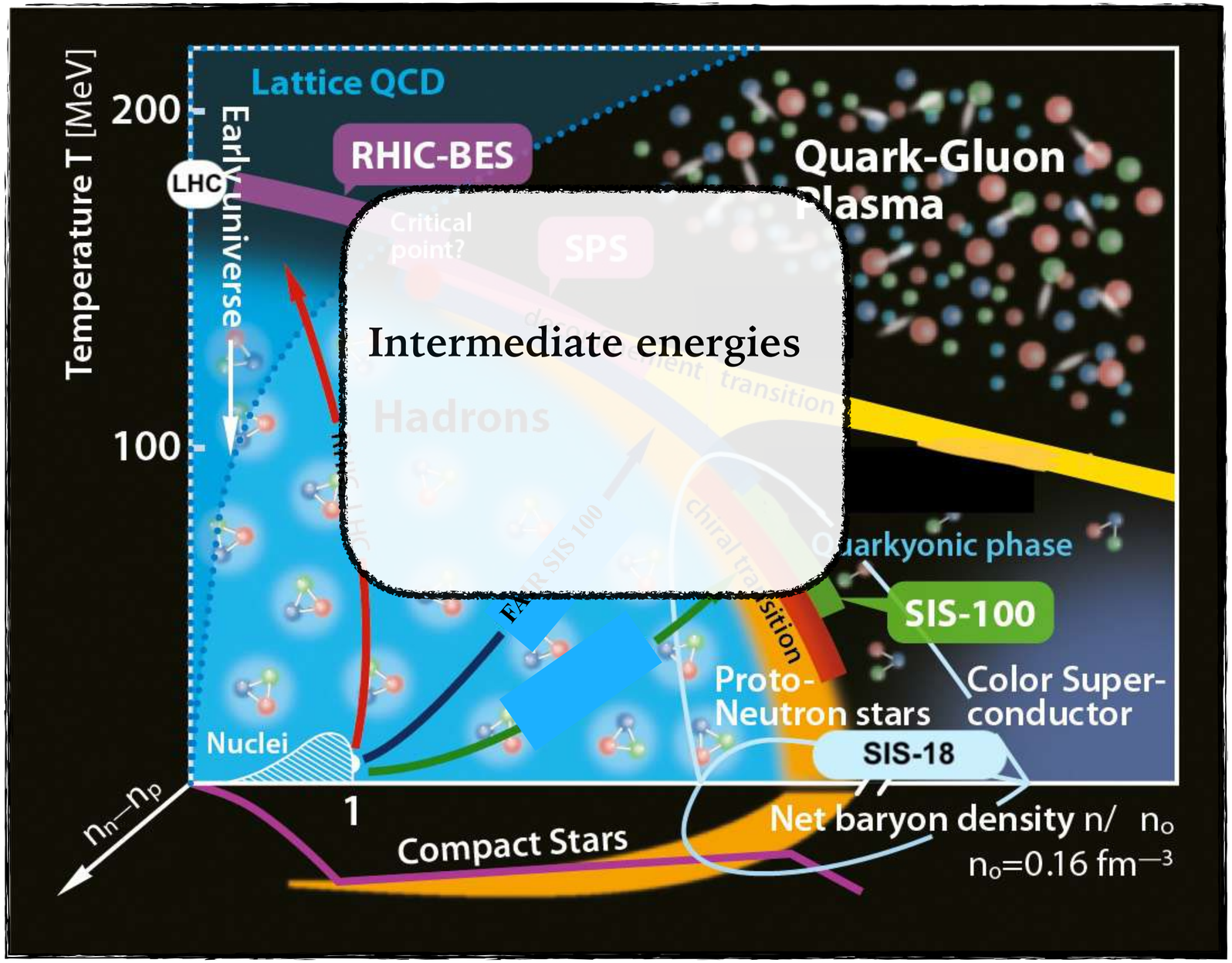

Program **B**eam **E**nergy **S**can

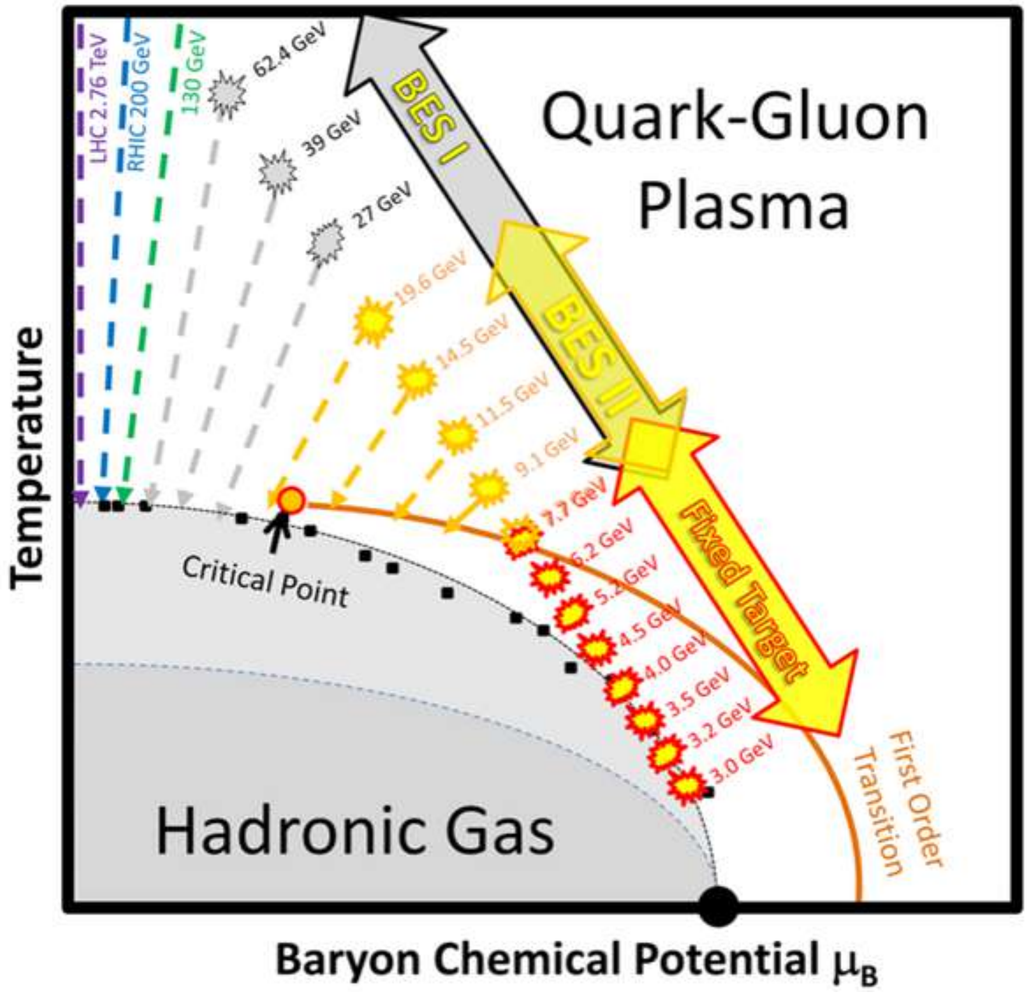

RHIC Top Energy: 200 GeV

p+p, p+Al, p+Au, d+Au, 3He+Au, Cu+Cu, Cu+Au, Ru+Ru, Zr+Zr, Au+Au, U+U

1. QCD at high energy density/temperature
2. Properties of QGP, EoS

Beam Energy Scan: Au+Au 7.7-62 GeV

1. Search for **turn-off** of **QGP** signatures
2. Search for signals of the **first-order phase transition**
3. Search for QCD **critical point**
4. Search for signals of **Chiral symmetry restoration**

Fixed-Target Program: Au+Au =3.0-7.7 GeV

High baryon density regime with 420-720 MeV

Identical pion femtoscopy

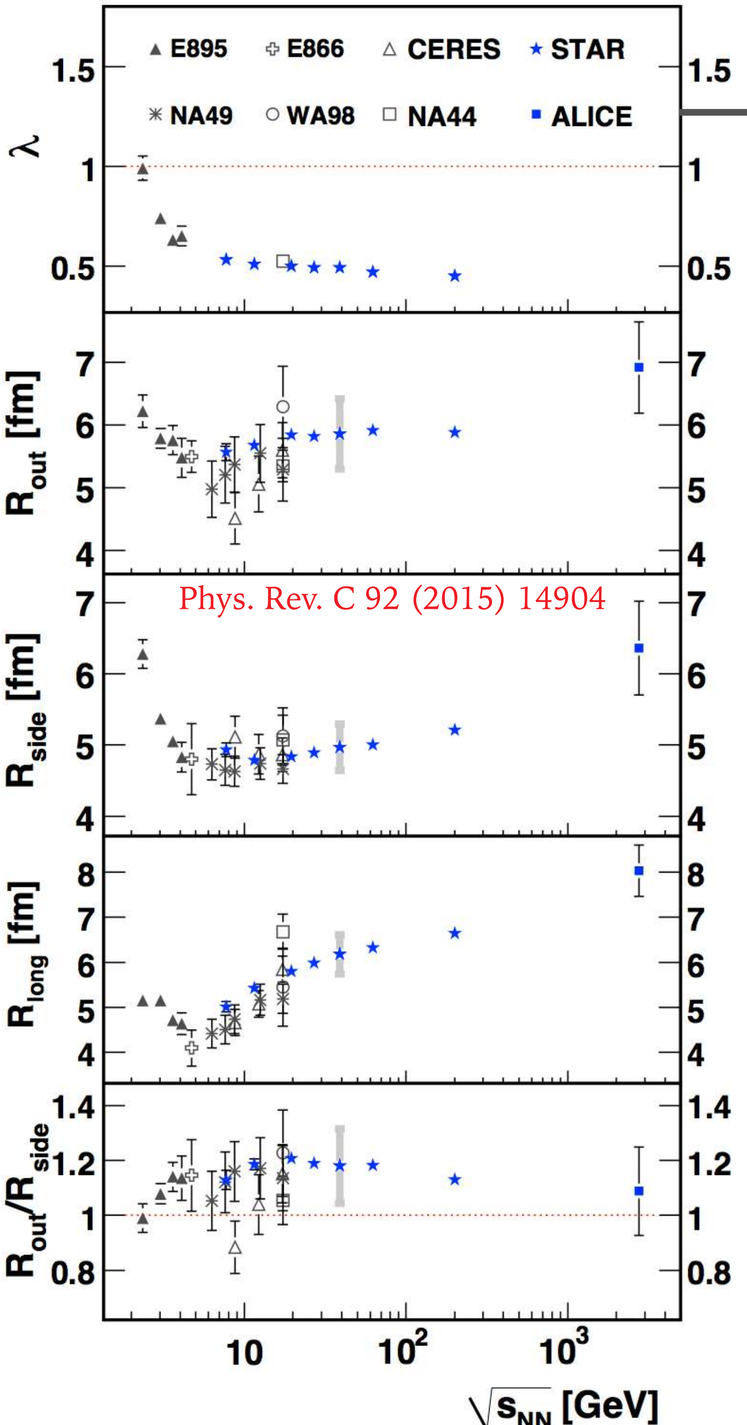

→ R_{side} spatial source evolution in the transverse direction

→ R_{out} related to spatial and time components

→ R_{out}/R_{side} signature of phase transition

→ $R_{out}^2 - R_{side}^2 = \Delta\tau^2 \beta_t^2$; $\Delta\tau$ – emission time

→ R_{long} temperature of kinetic freeze-out and source lifetime

$$C(\vec{q}) = (1-\lambda) + K_{Coul}(q_{inv})\lambda \times \exp\left(-q_o^2 R_o^2 - q_s^2 R_s^2 - q_l^2 R_l^2 - 2q_o q_s R_{os}^2 - 2q_o q_l R_{ol}^2\right)$$

HBT source sizes determined for wide range of collision energy;

Non-monotonic behavior seen in three directions

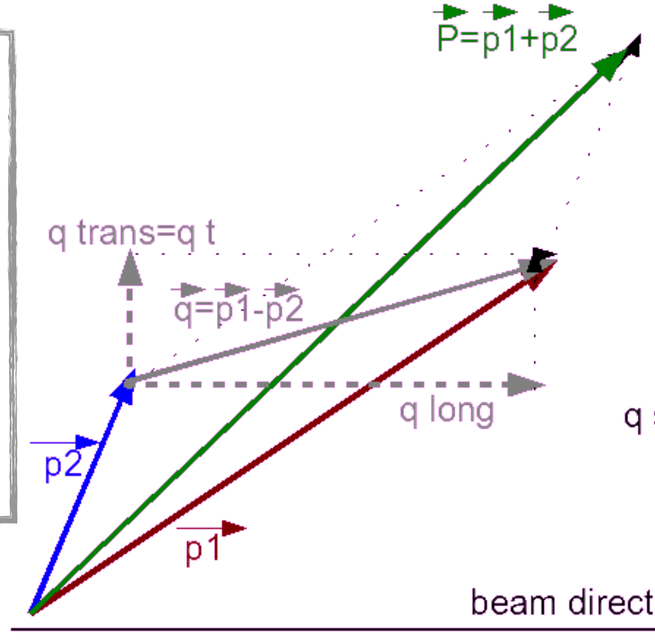

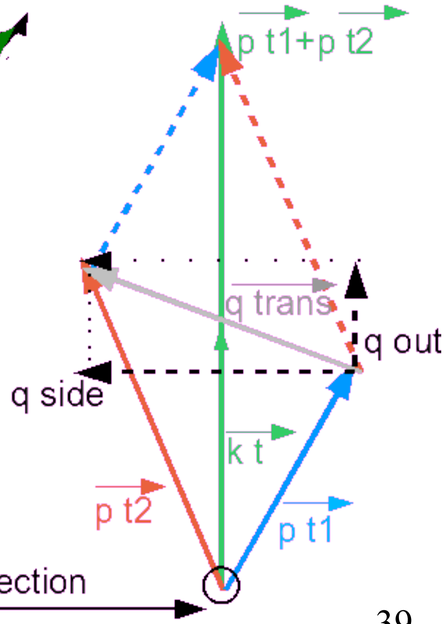

Identical pion femtoscopy

→ R_{side} spatial source evolution in the transverse direction

→ R_{out} related to spatial and time components

→ R_{out}/R_{side} signature of phase transition

→ $R_{out}^2 - R_{side}^2 = \Delta\tau^2 \beta_t^2$; $\Delta\tau$ – emission time

→ R_{long} temperature of kinetic freeze-out and source lifetime

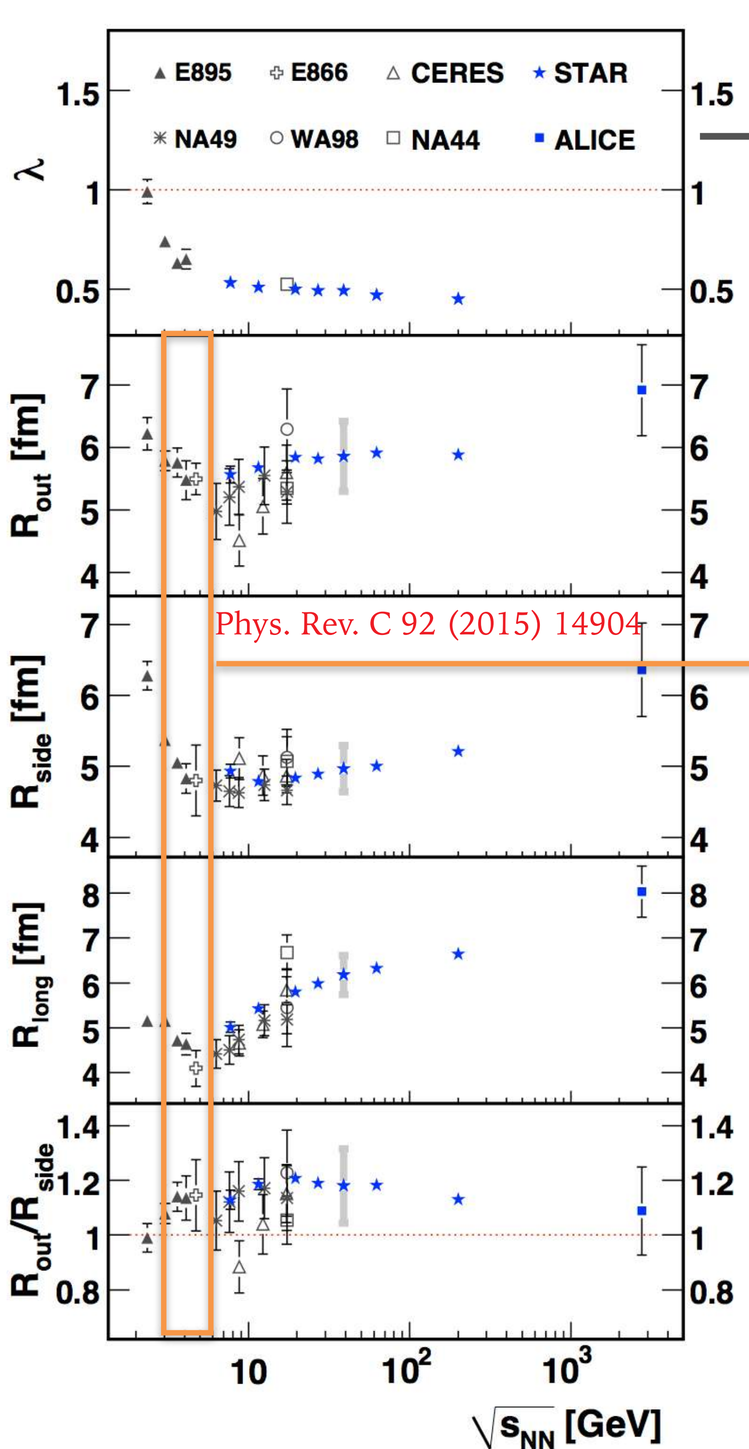

Phys. Rev. C 92 (2015) 14904

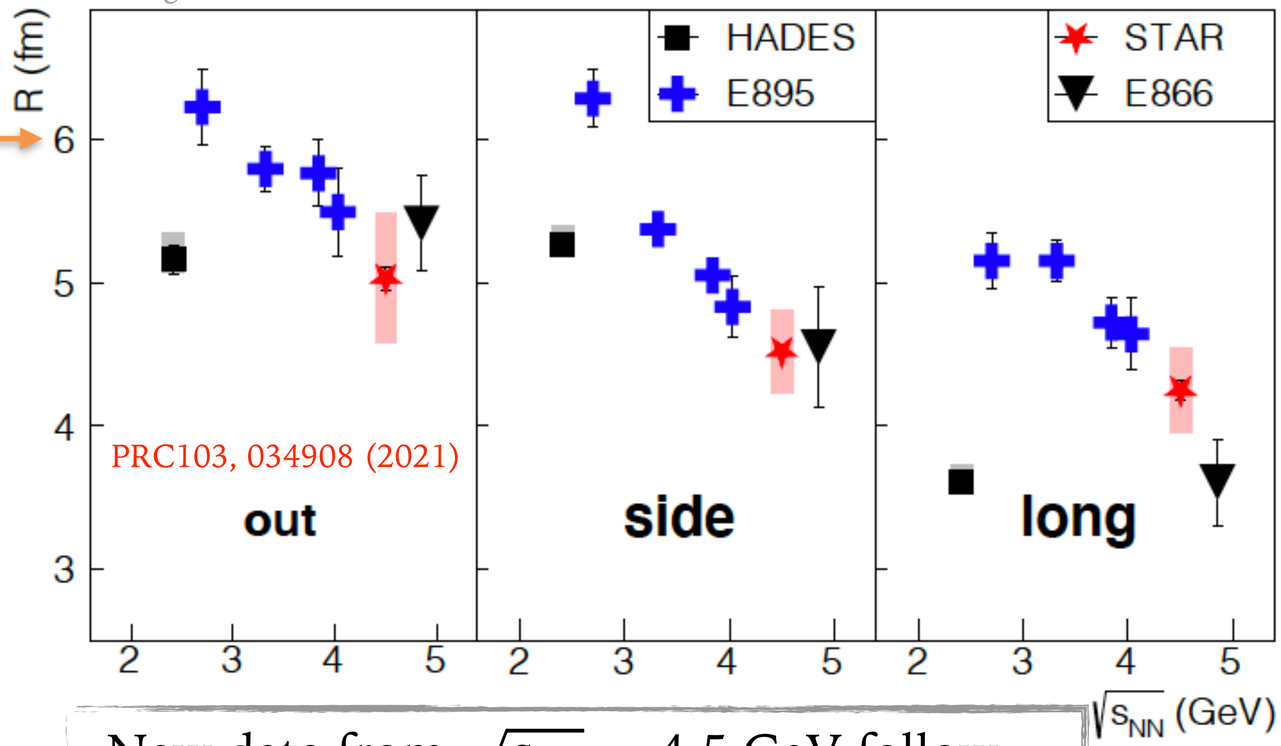

PRC103, 034908 (2021)

New data from $\sqrt{s_{NN}} = 4.5$ GeV follow trend observed for low collision energies

Identical pion femtoscopy

$$R_\mu^2(\Phi) = R_{\mu,0}^2 + 2\sum_{n=2,4,6\ldots} R_{\mu,n}^2 \cos(n\Phi) \qquad (\mu = o,s,l,ol)$$

$$R_\mu^2(\Phi) = R_{\mu,0}^2 + 2\sum_{n=2,4,6\ldots} R_{\mu,n}^2 \sin(n\Phi) \qquad (\mu = os)$$

$$\varepsilon_{PP} = \frac{\sqrt{(\sigma_y^2 - \sigma_x^2)^2 + 4\sigma_{xy}^2}}{\sigma_x^2 + \sigma_y^2}.$$

$$\varepsilon_F = \frac{\sigma_y'^2 - \sigma_x'^2}{\sigma_y'^2 + \sigma_x'^2} \approx 2\frac{R_{s,2}^2}{R_{s,0}^2}$$

$$\sigma_x^2 = \{x^2\} - \{x\}^2 \text{ and } \sigma_y^2 = \{y^2\} - \{y\}^2$$

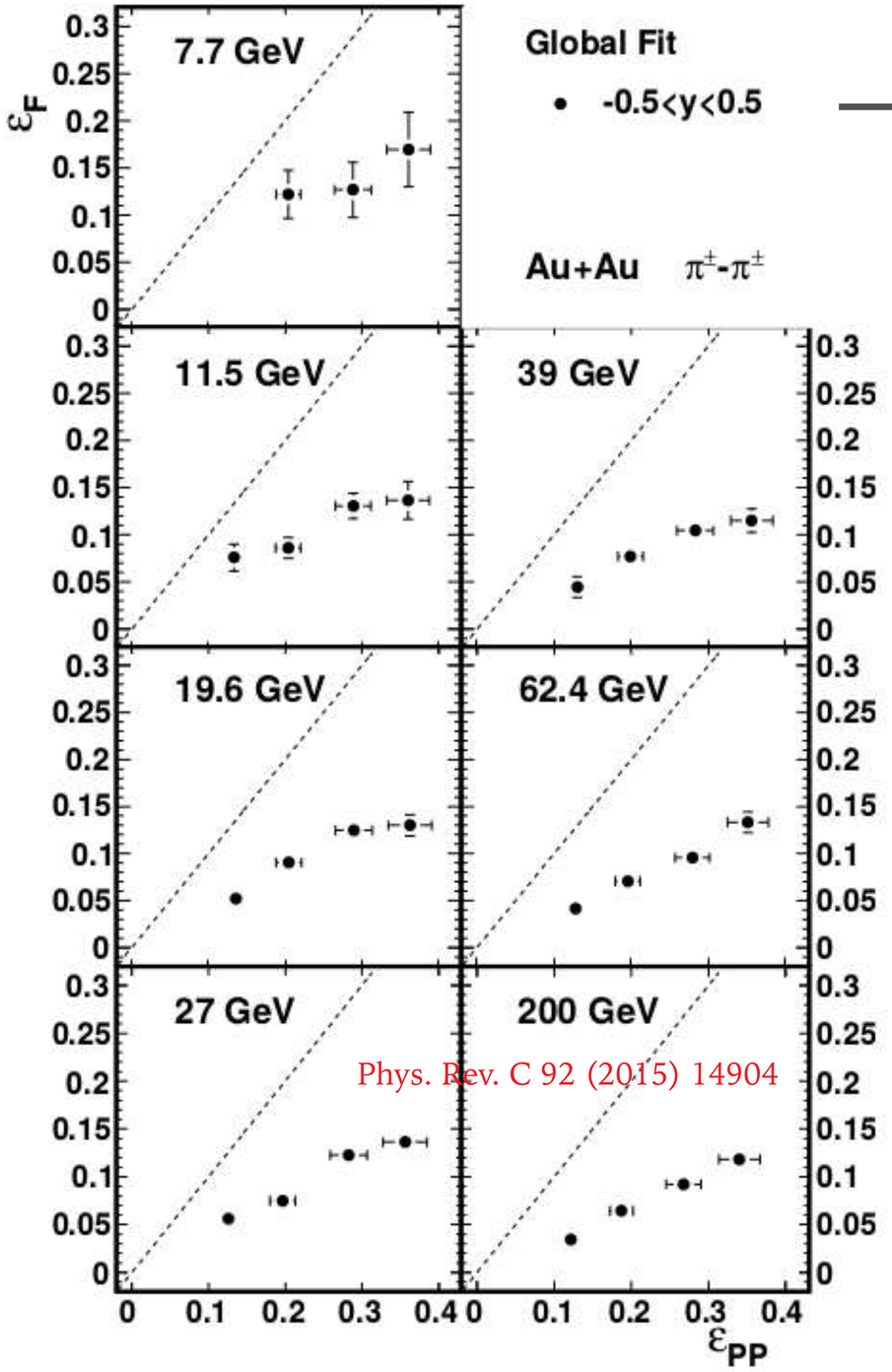

Phys. Rev. C 92 (2015) 14904

System evolves faster in the reaction plane

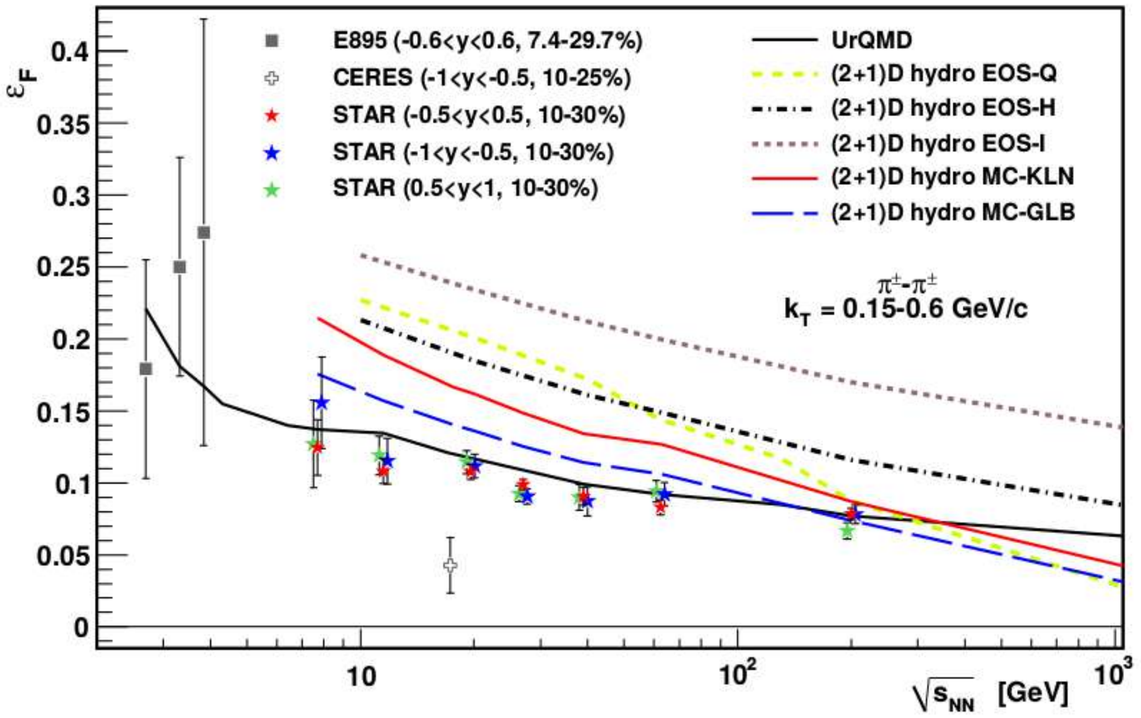

How to measure a phase transition?

$$R_{out}^2 - R_{side}^2 = \beta_t^2 \Delta\tau^2$$

Visible peak in $\frac{R_{out}}{R_{side}}(\sqrt{s_{NN}})$ near the $\sqrt{s_{NN}} \simeq 20$ GeV

QCD calculations predict a peak near to the QGP transition threshold - signature of **first-order phase transition?**

Theoretical attention from hydro and transport models needed

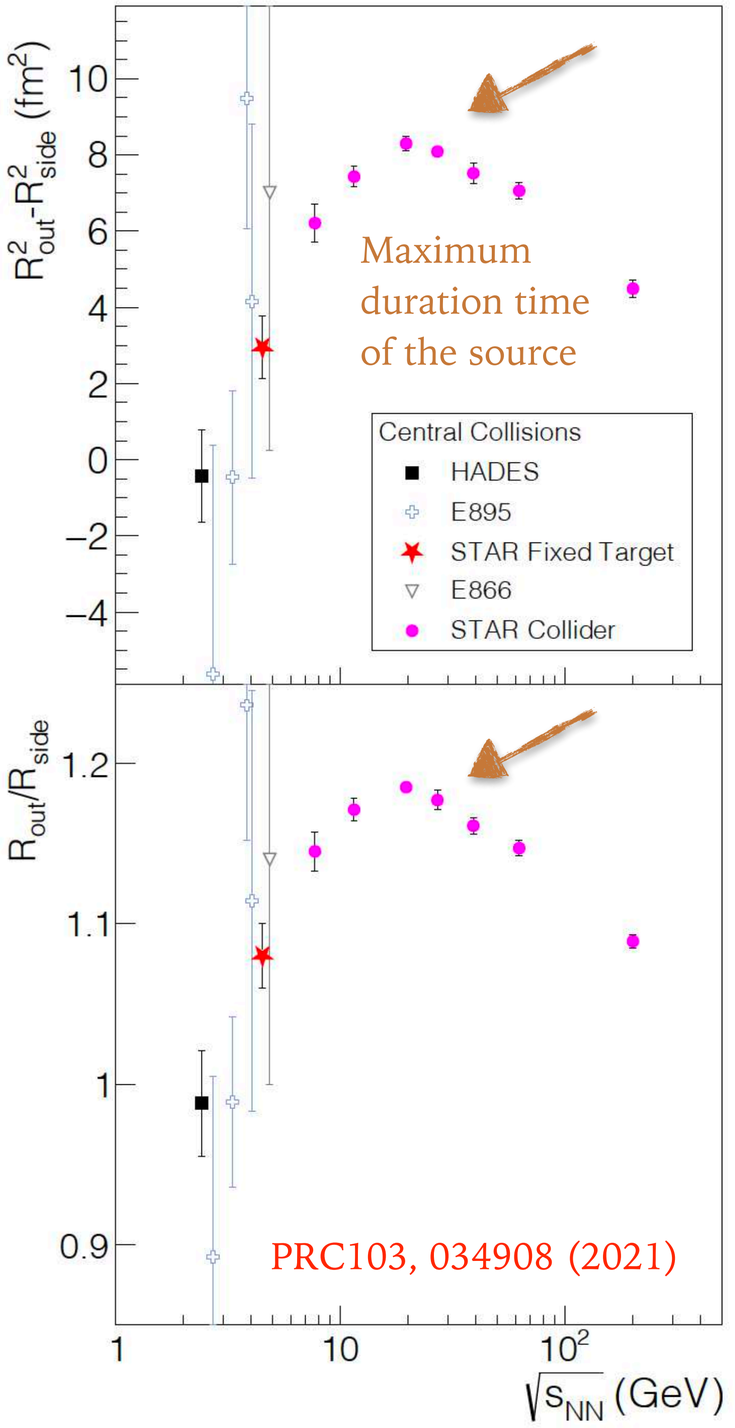

How to measure a phase transition?

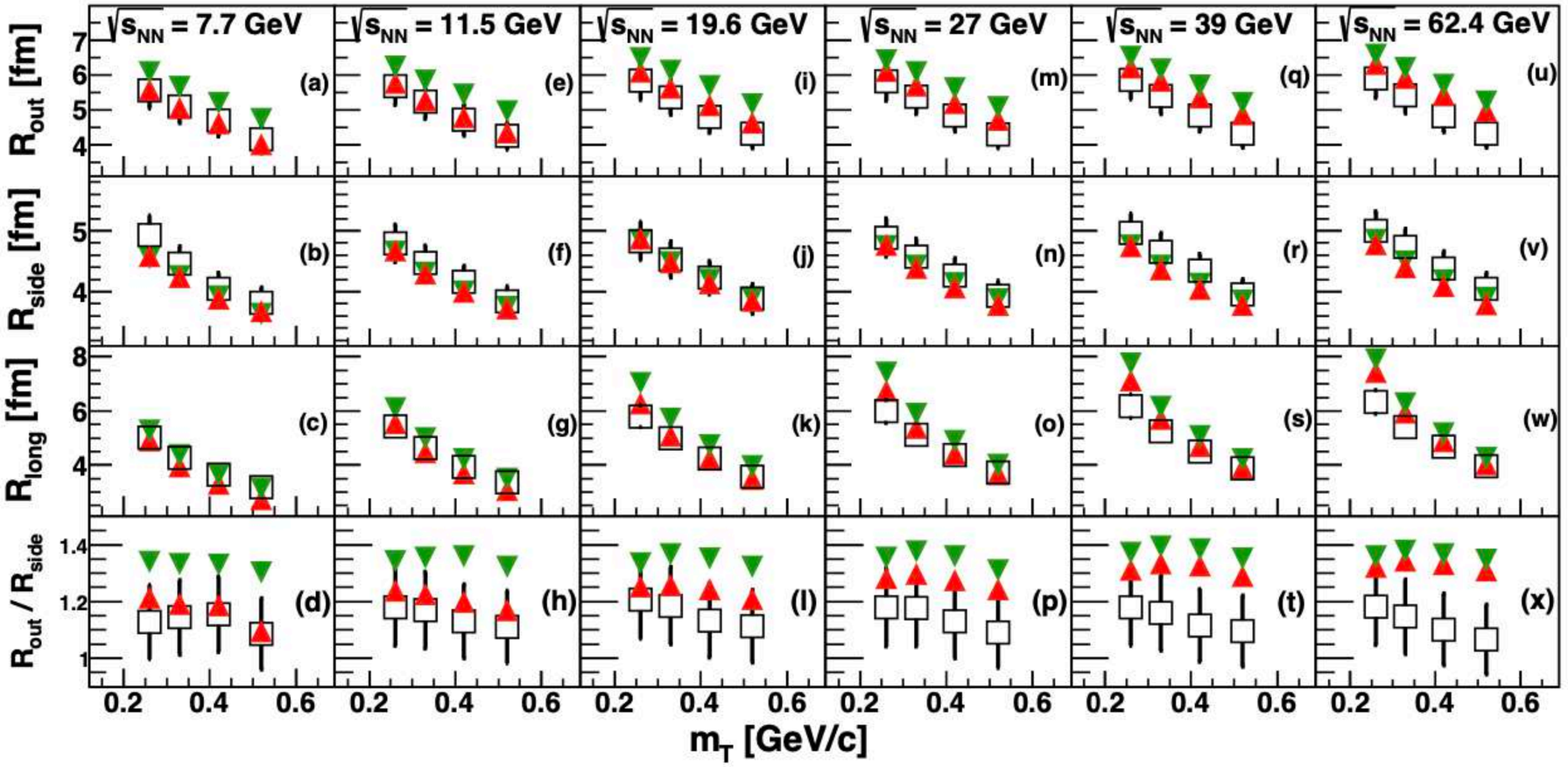

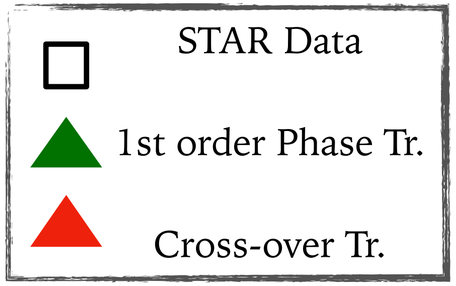

Phys.Rev. C96 (2017) no.2, 024911

vHLLE (3+1)-D viscous hydrodynamics: Iu. Karpenko, P. Huovinen, H. Petersen, M. Bleicher; Phys.Rev. C 91, 064901 (2015), arXiv:1502.01978, 1509.3751

HadronGas + Bag Model → 1st order PT ; P.F. Kolb, et al, PR C 62, 054909 (2000)

Chiral EoS → crossover PT (XPT); J. Steinheimer, et al, J. Phys. G 38, 035001 (2011)

Pre-thermal phase → Hydrodynamical phase → Hydronic cascades

UrQMD vHLEE UrQMD

vHLEE+UrQMD model verify **sensitivity of HBT measurements to the first-order phase transition**

Conclusions & Summary

Summary

- Descriptions of the interaction among antimatter (based on the simplest systems of anti-nucleons) determined.
- A quantitative verification of matter-antimatter symmetry in context of the forces responsible for the binding of (anti)nuclei.
- Scattering length is positive and favor $\Lambda - \Lambda$ bound state hypothesis
- Scattering length is positive and favor $p - \Omega$ bound state hypothesis
- Searched for $\Xi - \Xi$ bounds states have started
- Antonelli parametrization of $K_S^0 - K^{\pm}$ strong interactions favors $a_0(980)$ resonance as a tetraquark
- d-d CF described better by the model including coalescence
- Light nuclei are likely to be formed via coalescence
- Two-particle correlations are useful tool to explore unknown QCD phase diagram area

Back-up slides

Inside a neutron star

„The most efficient cooling mechanism of a NS by neutrino emission is the nucleonic electron direct Urca (DU) process (Lattimer et al., 1991) described by the equations:

$n \rightarrow p + e^- + \underline{\nu}_e$

$p + e^- \rightarrow n + \nu_e$

Frontiers in Astronomy and Space Sciences | www.frontiersin.org 1 March 2019 | Volume 6 | Article 13

$M_{NS} \approx 1 \div 2\ M_\odot$

$\rho \approx 3 \div 5\ \rho_0$

$\rho_0 \approx 2.8 \times 10^{14}$ g/cm^3

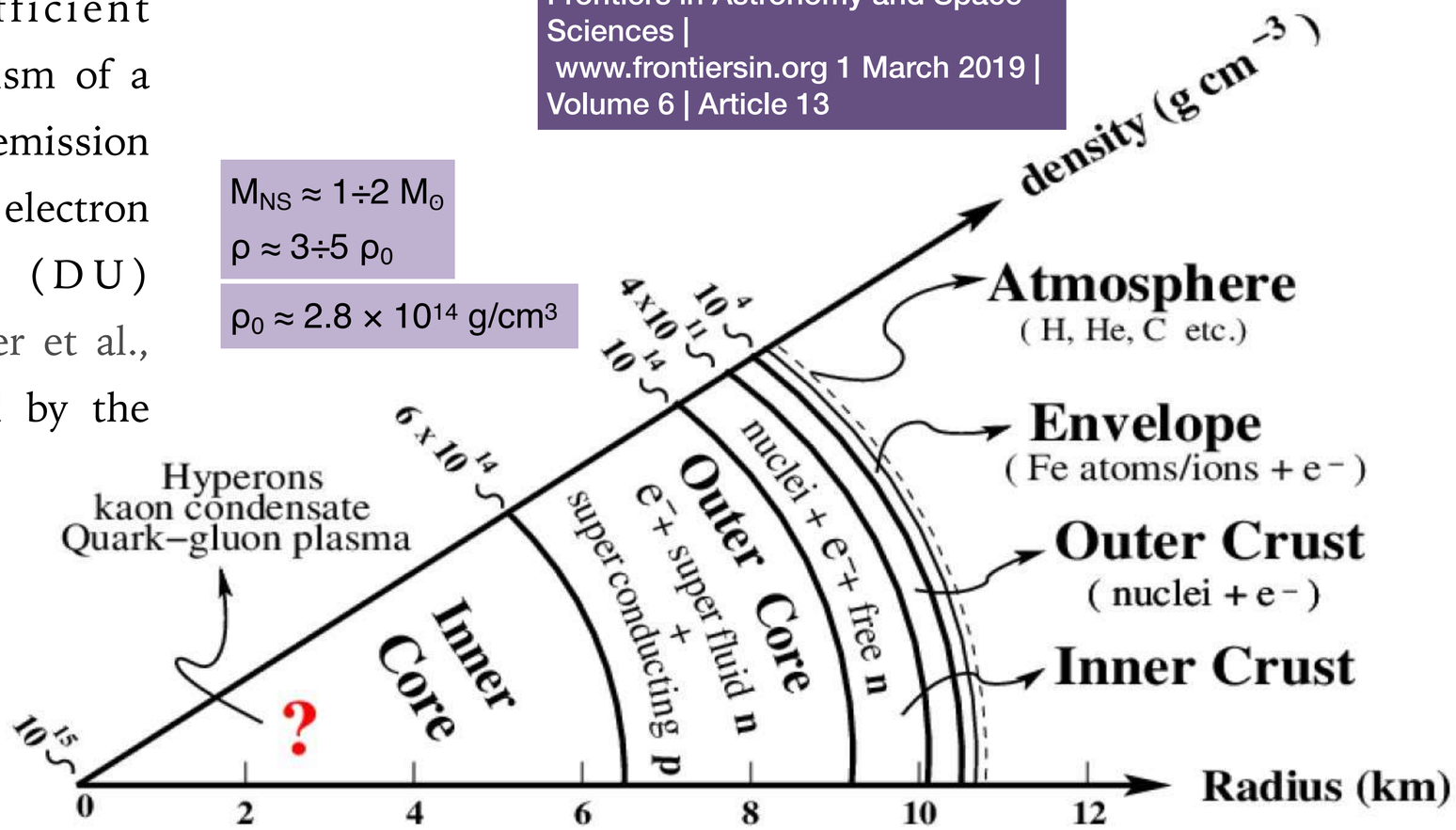

FIG. 1: Internal structure of a neutron star [2].

Role of Hyperons in Neutron stars, Ishfaq A. Rather1, M. Ikram1, and M. Imran1
1 Department of Physics, Aligarh Muslim University, Aligarh - 202002, INDIA

Strange hadronic matter in the inner core

The inner core of the neutron star is totally unknown. One of the most probable scenarios is that hyperons (baryons with strange quarks) appear at a density larger than (2–3) ρ_0

Λ hyperons, being free from Pauli exclusion principle by neutrons, are allowed to stay at the bottom of the attractive nuclear potential made by neutrons. When the kinetic energy of a neutron on the Fermi surface of the degenerate neutron matter exceeds the Λ-n mass difference of 176 MeV, it converts into a Λ hyperon via weak interaction.

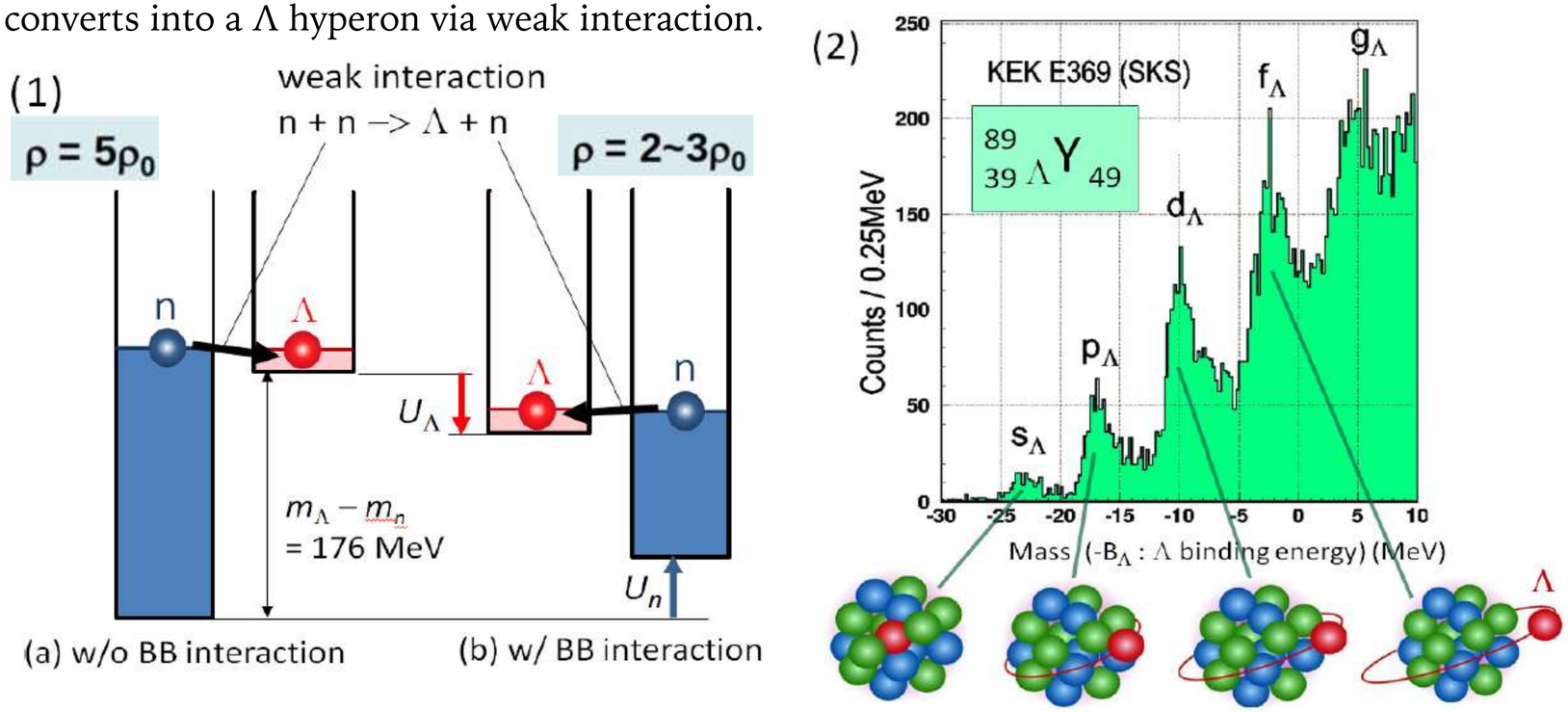

Fig. 3. (1) Energies of neutrons and Λ hyperons in high density neutron matter confined in the potential made by gravity. See text for details. (2) Excitation spectrum of a Λ hypernucleus $^{89}_{\Lambda}$Y via the (π^+,K^+) reaction on ^{89}Y target [6].

H. Tamura, JPS Conf Proc. 1, 011003 (2014)

Lednicky - Lyuboshitz model

Sov. Journ. Nucl. Phys. 35 (1982) 770

Complete description of two-particle correlations for small relative velocities including quantum statistics effects and interactions at the final states (Coulomb, strong)

Assumptions:

- independent emission,
- single-particle source,
- point emission sources;
- unpolarized particles;
- individual spin-state, momentum and position;
- Gaussian distribution of emission point's coordinates;
- s-wave component dominant in the description of FSI (valid for close relative velocities)
- Source size bigger than the range of interaction (~1fm)
- Smaller source sizes should include contribution of nuclear interaction)

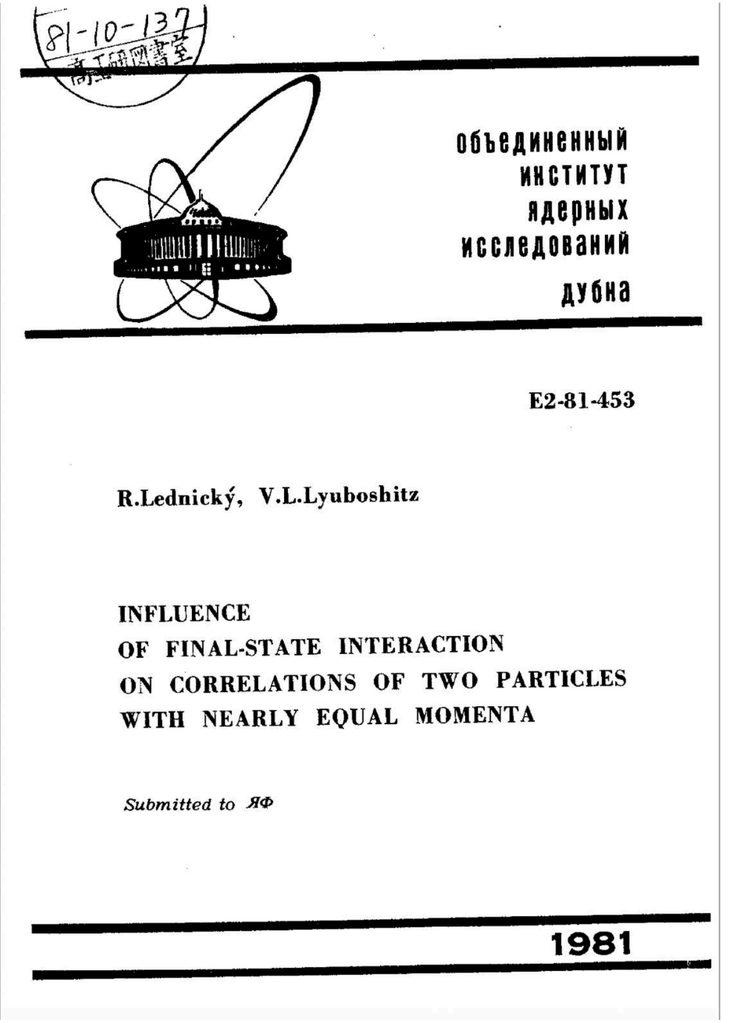

81-10-137

ОБЪЕДИНЕННЫЙ ИНСТИТУТ ЯДЕРНЫХ ИССЛЕДОВАНИЙ ДУБНА

E2-81-453

R.Lednický, V.L.Lyuboshitz

INFLUENCE OF FINAL-STATE INTERACTION ON CORRELATIONS OF TWO PARTICLES WITH NEARLY EQUAL MOMENTA

Submitted to ЯФ

1981

Lednicky - Lyuboshitz model

Sov. Journ. Nucl. Phys. 35 (1982) 770

Complete description of two-particle correlations for small relative velocities including quantum statistics effects and interactions at the final states (Coulomb, strong)

Assumptions:

- independent emission,
- single-particle source,
- point emission sources;
- unpolarized particles;
- individual spin-state, momentum and position;
- Gaussian distribution of emission point's coordinates;
- s-wave component dominant in the description of FSI (valid for close relative velocities)
- Source size bigger than the range of interaction (~1fm)
- Smaller source sizes should include contribution of nuclear interaction)

2. The correlation function (7) should be averaged over a space-time distribution of particle sources. The result is denoted as follows:

$$B(q,p) = \langle b_0(p_1,p_2)\rangle + \langle b_i(p_1,p_2)\rangle = B_0(q,p) + B_i(q,p). \qquad (11)$$

Below we consider in detail the correlations of two unpolarized neutrons. According to eq. (8), we have

$$B_0(q,p) = -\frac{1}{2}\langle\cos(qx)\rangle. \qquad (12)$$

Using formula (6) also inside the range of the interaction potential, eq. (9) yields

$$B_i(q,p) = \frac{1}{2}\{|f(k^*)|^2\langle|\Phi_{p_1p_2}(x)|^2\rangle + 2\mathrm{Re}[f(k^*)\langle\Phi_{p_1p_2}(x)\cos\tfrac{qx}{2}\rangle]\}. \qquad (13)$$

The nn-interaction amplitude in the effective range approximation is of the form /14/

$$f(k^*) = (\frac{1}{f_0} + \frac{1}{2}d_0k^{*2} - ik^*)^{-1}. \qquad (14)$$

According to the experimental data (see, e.g., /15/), the scattering length f_0 and the effective radius d_0 are equal to 17 fm * and 2.7 fm, respectively.

The neutron emission points are assumed to be independent and distributed according to the Gaussian law

* The data on neutron-proton scattering yield the singlet scattering length equal to 23.7 fm /14/. Such a violation of isotopic invariance is not yet completely clarified.

Formalizm opisu korelacji dwucząstkowych

HZ, Monografia habilitacyjna, 2018

4.1.1 Pary nieoddziałujących identycznych bozonów, np. (π^+, π^+)

Przyjmijmy na początek, że emitowane cząstki są bozonami (np. pionami), a więc cząstkami o spinie $s = 0$. Jeśli rozpatrywane pary cząstek stanowią piony identyczne, czyli nierozróżnialne, to opisując ich funkcje falowe w postaci fal płaskich oraz uwzględniając warunki statystyki kwantowej Bosego-Einsteina (BE), czyli w tym przypadku symetryzację funkcji falowej, mamy dla pary identycznych pionów

$$P_2^C(p_1, p_2) = \int d^4x_1 d^4x_2 W_2(x_1, p_1; x_2, p_2) |\frac{1}{\sqrt{2}}(e^{ip_1x_1+ip_2x_2} + e^{ip_1x_2+ip_2x_1})|^2 \quad (4.3)$$

Mając na uwadze, że

$$\frac{1}{\sqrt{2}}(e^{ip_1x_1+ip_2x_2} + e^{ip_1x_2+ip_2x_1})|^2 = 1 + cos(qx) \quad (4.4)$$

gdzie q jest różnicą pędów $q = p_1 - p_2$, a x jest różnicą współrzędnych $x = x_1 - x_2$, otrzymujemy wyrażenie:

$$P_2^C(p_1, p_2) = \int d^4x_1 d^4x_2 W_2(x_1, p_1; x_2, p_2)[1 + cos(qx)] \quad (4.5)$$

Zgodnie z sugestią Kopyłowa i Podgoreckiego [91, 92], zdefiniujmy teraz funkcję korelacyjną $C_2(p_1, p_2)$ jako stosunek prawdopodobieństwa emisji cząstek w przypadku kiedy efekty statystyki kwantowej są włączone („on"), czyli $P_2^C(p_1, p_2)$, do przypadku, kiedy są wyłączone („off") czyli $P_2(p_1, p_2)$. Mamy więc

$$C_2(p_1, p_2) = \frac{\int d^4x_1 d^4x_2 W_2(x_1, p_1; x_2, p_2)[1 + cos(qx)]}{\int d^4x_1 d^4x_2 W_2(x_1, p_1; x_2, p_2)} \quad (4.6)$$

co inaczej może być także zapisane w postaci

$$C_2(p_1, p_2) = 1 + < cos(qx) > \quad (4.7)$$

gdzie uśrednienie przeprowadza się po obszarze emisji. Jak widać, dla małych pędów względnych zwiększa się populacja par bozonów i dla zdążającej do zera różnicy pędów q, funkcja korelacyjna zbiega do wartości 2.0. Szybkość zbiegania zależy od rozkładu gęstości źródeł w obszarze emitującym cząstki. Im obszar ten jest większy, tym zakres efektu korelacyjnego jest węższy, co wynika także bezpośrednio z zasady nieoznaczoności.

Formalizm opisu korelacji dwucząstkowych

HZ, Monografia habilitacyjna, 2018

4.1.2 Pary nieoddziałujących fermionów identycznych, np. (p,p) lub (n,n)

W przypadku pary identycznych nukleonów, np. protonów lub neutronów, musimy uwzględnić, że są one fermionami i mogą występować w stanach: singletowym, $S = 0$ oraz trypletowym, $S = 1$, a populacje tych stanów w przypadku niespolaryzowanej emisji są odpowiednio: 1/4 i 3/4. Funkcja korelacyjna będzie mieć wtedy postać [93, 94]:

$$C_2(p_1, p_2) = \frac{1}{4}[1 + < cos(qx) >] + \frac{3}{4}[1 - < cos(qx) >] = 1 - \frac{1}{2} < cos(qx) > \quad (4.8)$$

Jak widać, w obszarze małych pędów względnych zmniejsza się populacja par fermionów i dla zdążającej do zera wartości , funkcja korelacyjna zbiega do wartości 1/2.

4.1.3 Przypadek cząstek spolaryzowanych

Kiedy mamy do czynienia z emisją cząstek spolaryzowanych, to populacje stanów zależeć będą od stopnia polaryzacji określonej przez wektor polaryzacji P_n. Mamy wtedy populację stanów: singletowego (ρ_0) i trypletowego (ρ_1):

$$\rho_0 = \frac{1}{4}(1 - P_n^2) \quad (4.9)$$

$$\rho_1 = \frac{1}{4}(3 + P_n^2) \quad (4.10)$$

Funkcja korelacyjna w takim przypadku określona jest wzorem:

$$C_2(p_1, p_2) = 1 - [\frac{1 + P^2}{2}] < cos(qx) > \quad (4.11)$$

Warto zauważyć, że w przypadku całkowitej polaryzacji ($P^2 = 1$) cząstki mogą być wyłącznie w stanie trypletowym, a funkcja korelacyjna wynosi wtedy zero dla zerowej różnicy pędów q.

Formalizm opisu korelacji dwucząstkowych

HZ, Monografia habilitacyjna, 2018

4.1.4 Pary nieidentycznych oddziałujących barionów, np. (n,p)

Omawiane wyżej efekty statystyk kwantowych nie mają odniesienia do par cząstek nieidentycznych, np. neutron - proton (n,p). Jednakże zarówno cząstki identyczne, jak i nieidentyczne podlegają wzajemnemu oddziaływaniu w stanie końcowym, które także zależy od czasowo-przestrzennych współrzędnych punktów ich emisji. Wszystkie hadrony podlegają oddziaływaniu silnemu, wszystkie cząstki obdarzone ładunkiem elektrycznym - kulombowskiemu. Dla uwzględnienia oddziaływania w stanie końcowym zamieniamy fale płaskie z powyższych rozważań przez amplitudę Bethe-Salpetera [93, 94, 95, 96]:

$$e^{ip_1x_1+ip_2x_2} \to \psi^S_{p_1,p_2}(x_1,x_2) = e^{ip_1x_1+ip_1x_2} + \varphi^{(S)}_{p_1,p_2}(x_1,x_2) \tag{4.12}$$

gdzie $\varphi^{(S)}_{p_1,p_2}(x_1,x_2)$ jest falą rozproszoną. W takim przypadku funkcja korelacyjna przyjmuje postać:

$$C_2(p_1,p_2) = \rho_0 < |\psi^{(0)}_{p_1p_2}(x)|^2 > + \rho_1 < |\psi^{(1)}_{p_1p_2}(x)|^2 > \tag{4.13}$$

gdzie $\psi^{(s)}_{p_1,p_2}(x)$ jest otrzymana z amplitudy Bethe-Salpetera po separacji ruchu układu środka masy pary

$$\psi^{(S)}_{p_1p_2}(x_1,x_2) = e^{iPX}\psi^{(S)}_{p_1p_2}(x) \tag{4.14}$$

Pęd i położenie układu środka masy pary określamy jako: $P = p_1 + p_2$ oraz $X = [(p_1P)x_1 + (p_2P)x_2]/P^2 = \{X_0, R\}$. Poprzez taką faktoryzację oddzielamy ruch układu jako całości od wzajemnego oddziaływania rozpatrywanych cząstek.

Populacje stanów: singletowego (ρ_0) i trypletowego (ρ_1) dla pary (n,p) mamy:

$$\rho_0 = \frac{1}{4}(1 - \vec{P}_n\vec{P}_n) \tag{4.15}$$

$$\rho_1 = \frac{1}{4}(3 + \vec{P}_n\vec{P}_n) \tag{4.16}$$

Przechodzimy teraz do układu środka masy pary, który oznaczać będziemy gwiazdką $(*)$. Zdefiniujmy $x^* = (r^*, t^*)$ w tym układzie. Można pokazać, że jeśli $|t^*| << mr^{*2}$, to uzasadnione jest założenie jednoczesności emisji cząstek w ich układzie środka masy i amplituda $\psi^{(S)}_{p_1,p_2}(x^*)$ może być zamieniona przez funkcję falową $\psi^{(S)}_{-k^*}(r^*)$, która opisuje względny ruch cząstek i ich rozpraszanie w kinematyce odwrotnego biegu czasu, zaś przy $r^* \to \infty$ jest superpozycją fali płaskiej i rozchodzącej się fali kulistej:

$$\psi^{(S)}_{-k^*}(\vec{r^*}) \to e^{-i\vec{k^*}\vec{r^*}} + f^{(S)}(\vec{k^*})\frac{e^{-ik^*r^*}}{r^*} \tag{4.17}$$

gdzie $k^* = \sqrt{-q^2}/2$, a $f^{(S)}$ jest długością rozpraszania i dla układu (n,p) wynosi: $ff^{(0)}(0) = 23.7\,\text{fm}$ oraz $ff^{(1)}(0) = -5.4\,\text{fm}$. W rezultacie, dla typowych rozmiarów: $r_0, c\tau_0 \approx (2 \div 3)\,\text{fm}$ mamy $C_2(p_1 = p_2) \approx 10$, a więc korelacje są bardzo silne.

Formalizm opisu korelacji dwucząstkowych

HZ, Monografia habilitacyjna, 2018

4.1.5 Pary oddziałujących cząstek identycznych

Najogólniejszy przypadek dotyczy spolaryzowanych fermionów - oddziałujących cząstek identycznych o niezerowych spinach. Mamy wtedy do czynienia zarówno z efektami statystyki kwantowej, jak i z oddziaływaniem w stanie końcowym. Amplituda Bethe-Salpetera przyjmuje wtedy postać:

$$C_2(p_1,p_2) = \frac{1}{4}(1-\vec{P_n^2}) < |\frac{1}{\sqrt{2}}(\psi^{(0)}_{p_1p_2}(x) + \psi^{(0)}_{p_2p_1}(x))|^2 > + \frac{1}{4}(3+\vec{P_n^2}) < |\frac{1}{\sqrt{2}}(\psi^{(1)}_{p_1p_2}(x) + \psi^{(1)}_{p_2p_1}(x))|^2 > \quad (4.18)$$

Warto zauważyć, że w zakresie małych pędów względnych (małe wartości k^*) dominuje oddziaływanie silne w fali-s, i uczestniczy tylko w singletowej kombinacji spinowej (dwa identyczne nukleony w stanie fali-s nie mogą mieć spinów równoległych, tj. być w stanie trypletowym). Kiedy więc $|P_n| \approx 1$, to korelacja wynikająca z oddziaływania silnego znika. Efekt ten w zasadzie mógłby być wykorzystany do badania stanów polaryzacyjnych emitowanych nukleonów, chociaż praktycznie byłoby to trudne w realizacji. Funkcja korelacyjna dla cząstek niespolaryzowanych, jak również dla bozonów, to po prostu uproszczone warianty równ. 4.18 i podanych wcześniej wzorów.

Nonidentical particle correlations

Like-sign 0-10% @ Au+Au 39

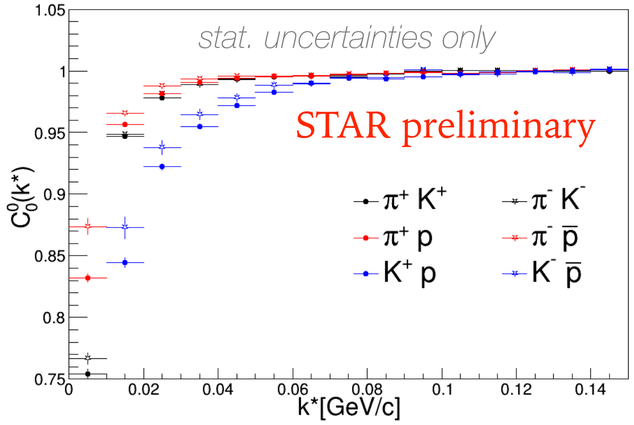

Determined by Coulomb Interactions

Unlike-sign 0-10% @ Au+Au 39 GeV

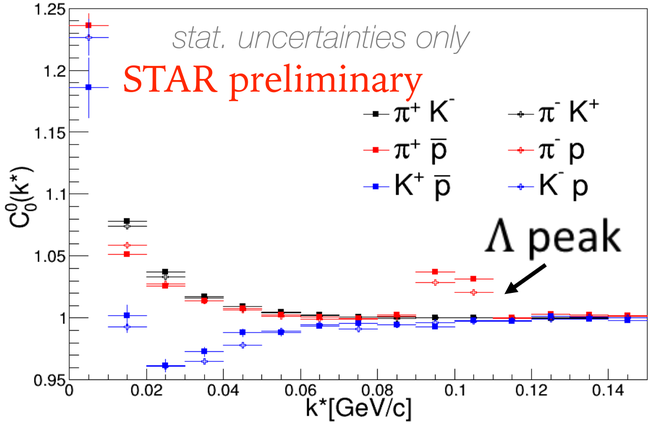

Determined by full FSI: Coulomb and Strong interactions (kaon-proton)

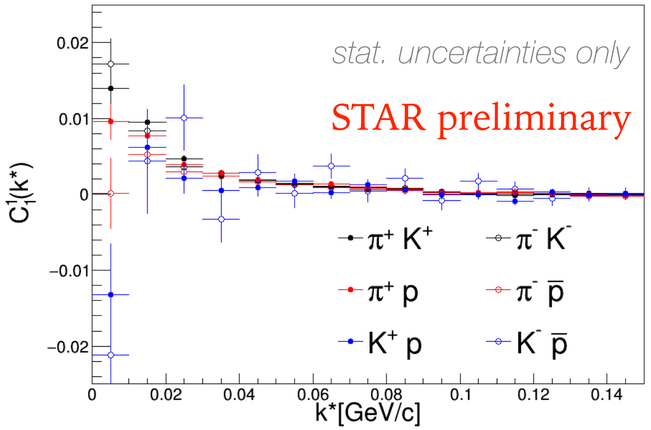

Nucl. Phys. A 982 (2019), 359-362

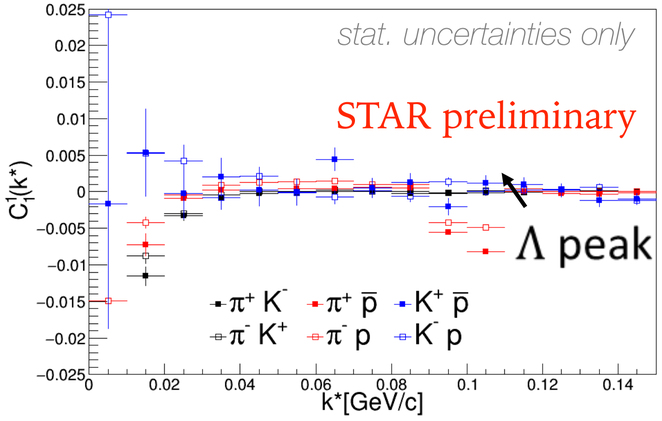

Heavier directed towards edge of the source.
Heavier particles freeze-out earlier

Phys. Rev. C81:064906 2010

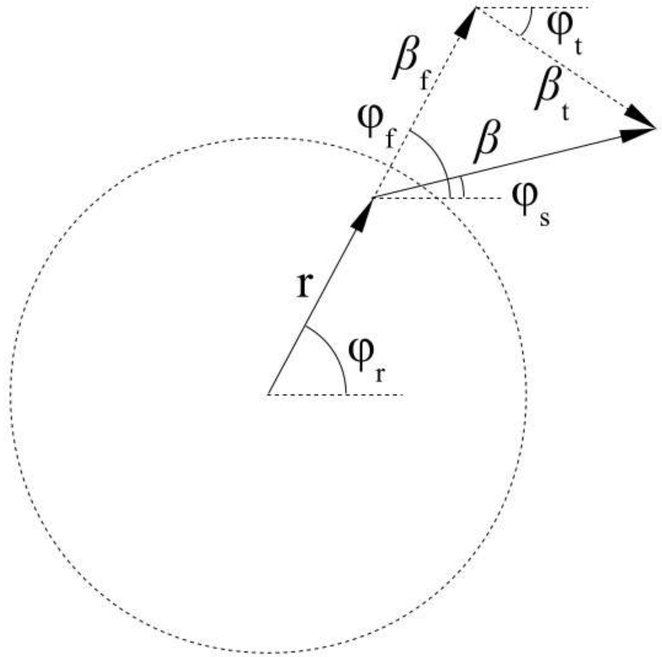

$$\langle x_{out} \rangle = \frac{\langle r \beta_f \rangle}{\left\langle \sqrt{\beta_t^2 + \beta_f^2} \right\rangle} = \frac{r_0 \beta_0 \beta}{\beta_0^2 + T/m_t},$$

$\beta_t \sim 1/m_T$ - smaller for heavier particles